Perspectives on Endoscopic Functional Photoacoustic Microscopy

Shuo Yang[1] and Song Hu[1,*]

[1]*Department of Biomedical Engineering, Washington University in St. Louis, St. Louis, Missouri, 63130, USA*

*Corresponding author: songhu@wustl.edu

Abstract

Endoscopy, enabling high-resolution imaging of deep tissues and internal organs, plays an important role in basic research and clinical practice. Recent advances in photoacoustic microscopy (PAM), demonstrating excellent capabilities in high-resolution functional imaging, have sparked significant interest in its integration into the field of endoscopy. However, there are challenges in achieving functional PAM in the endoscopic setting. This Perspective article discusses current progress in the development of endoscopic PAM and the challenges related to functional measurements. Then, it points out potential directions to advance endoscopic PAM for functional imaging by leveraging fiber optics, microfabrication, optical engineering, and computational approaches. Finally, it highlights emerging opportunities for functional endoscopic PAM in basic and translational biomedicine.

I. Introduction

Providing detailed structural, functional, and molecular insights into deep tissues and organs, endoscopy plays a crucial role in both basic research and clinical practice[1,2]. While non-invasive imaging technologies, including X-ray computed tomography (CT), magnetic resonance imaging (MRI), positron emission tomography (PET), and ultrasonography, can also image internal tissues and organs, endoscopy offers higher resolution and more diverse contrasts[2]. Commonly used endoscopic techniques are based on white light, ultrasound (US), optical coherence tomography (OCT), and fluorescence imaging. White-light endoscopy is easy to use, but lacks depth information[2,3]. Ultrasound endoscopy penetrates centimeters of tissue, but has limited resolution (>100 μm)[4]. OCT endoscopy, conversely, offers microscopic resolution, but penetrates only 1–2 millimeters[5]. Moreover, both US and OCT primarily provide structural information. Multi-photon fluorescence endoscopy, although offering cellular-level resolution and molecular contrast, has limited field of view and imaging speed[6].

Photoacoustic imaging (PAI), combining the advantages of light and ultrasound[7,8], holds great potential to bridge the gaps in existing endoscopic techniques and has attracted increasing attention in recent years (Fig. 1a). Optically, PAI provides unique absorption contrasts that reveal the structural, functional, and molecular information of biological tissues. Ultrasonically, PAI benefits from reduced tissue scattering and absorption compared to pure optical imaging, enabling depth-resolved, deep-tissue imaging with improved spatiotemporal resolution and extended field of view. In particular, photoacoustic microscopy (PAM), a major embodiment of PAI, offers multi-contrast imaging at the microscopic level (Fig. 1b)[9]. Recent advances in endoscopic PAM have demonstrated various preclinical (Fig. 1c) and clinical (Fig. 1d) applications[2]. However, only a small fraction of the existing work (~3%) presents functional imaging, highlighting the need for further development in this area.

Previous articles have comprehensively reviewed the technical advances[1,2,10] and applications[11] of endoscopic PAM in general. In contrast, this Perspective article focuses on the limitations of current endoscopic PAM techniques in functional imaging and provides insights into future directions. Specifically, the first section summarizes current progress on endoscopic PAM, with an emphasis on the probe design and construction. The second section discusses the technical limitations of functional imaging

in endoscopic PAM settings. The third section highlights various strategies that have the potential to address these limitations, by leveraging recent advances in fiber optics, microfabrication, optical engineering, and computational imaging. Finally, this article concludes by introducing potential opportunities for endoscopic functional PAM.

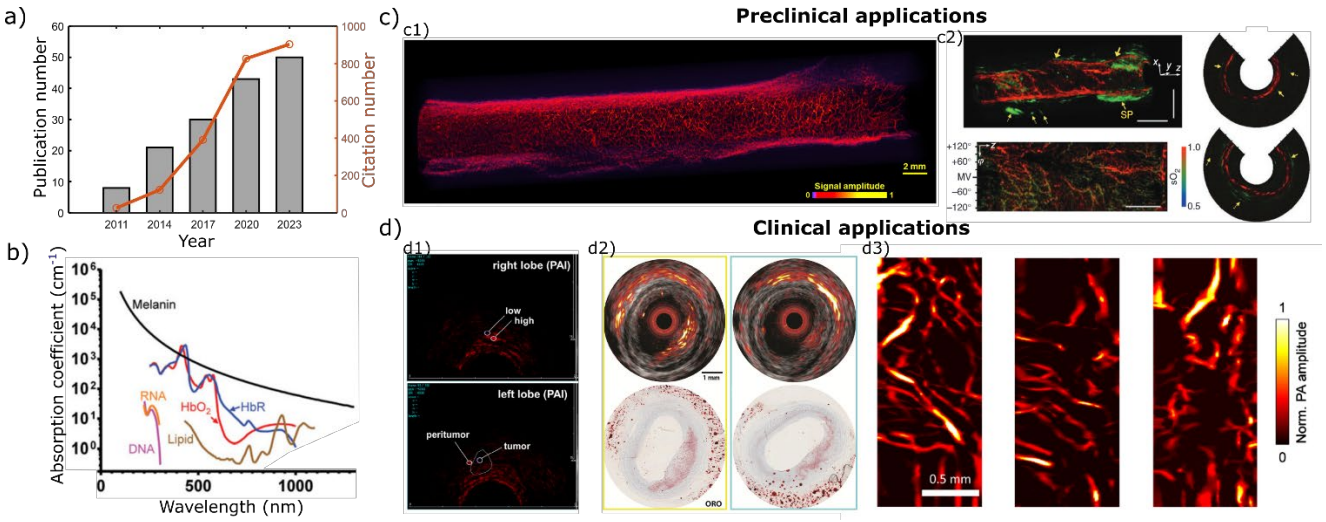

FIG.1. Advances in endoscopic photoacoustic microscopy (PAM). a) Publication and citation numbers from 2011 to 2023, searched with the keywords of "photoacoustic" and "endoscope/endoscopy" on the Web of Science. b) Absorption spectra of representative endogenous chromophores[9]. Reprinted with permission from [9] Copyright 2024 Wiley. c) Representative endoscopic PAM images acquired in animal models: c1) structural image of the 3D microvascular in a rat colorectum[12]; c2) blood oxygenation (sO_2) map in a rat colon[13]. Reprinted with permission from [12] Copyright 2024 Optica Publishing Group. Reprinted with permission from [13] Copyright 2024 Springer Nature. d) Representative clinical applications of endoscopic PAM: d1) differentiating normal and tumor tissues in a patient with prostate cancer[14]; d2) detecting atherosclerotic plaque in a human coronary artery with lipid contrast[15]; d3) examining the cervical remodeling in patients at different stages of pregnancy[16]. Reprinted with permission from [14] Copyright 2024 Elsevier. Reprinted with permission from [15] Copyright 2024 Optica Publishing Group. Reprinted with permission from [16] Copyright 2024 SPIE.

II. Current progress on endoscopic PAM

i. Biomedical applications of endoscopic PAM

Endoscopic PAM has shown great promise in both preclinical and clinical settings (Fig. 1c-d). In gastrointestinal imaging[13,13,17–26,26,27], it enables label-free microvascular imaging, facilitating diagnosis of diseases in the gastrointestinal tract. By visualizing abnormal angiogenesis, endoscopic PAM enhances the detection of colorectal cancer compared to traditional colonoscopy[28]. By assessing blood oxygenation, it provides valuable functional insights into Crohn's disease, an inflammatory bowel disease[23]. Moreover, endoscopic PAM has shown great promise in assessing the treatment response of rectal cancer[29]. In intravascular imaging[15,30–44], endoscopic PAM can characterize atherosclerotic plaques by identifying lipid-rich contents, which are prone to rupture and may lead to cardiovascular events[43]. In urology[14,45–47], endoscopic PAM can detect prostate cancer by measuring changes in the microvascular density that are typically associated with malignant growth[14] and visualize neurovascular bundles during radical prostatectomy[47]. In gynecology[16,48–52], endoscopic PAM has shown potential in screening the ovarian cancer by detecting subtle changes in the vascular structure and tissue oxygenation that are indicative of tumor presence or progression[48,50].

Also, it can examine cervical remodeling by identifying changes in the microvascular density[16]. These applications underscore the transformative potential of endoscopic PAM across various medical fields.

ii. Application-specific design and construction of endoscopic PAM probe

There are two typical configurations of endoscopic PAM, forward viewing and side viewing. The forward-viewing endoscopic PAM is mostly used for surgical guidance, such as laparoscopy[53] and breast tumor screening[54]. In contrast, the side-viewing configuration is widely adopted to examine the inner wall of tubular organs, such as the rectum, esophagus, and blood vessel[1]. Different applications impose specific requirements on the size of the endoscopic PAM probe to ensure fitness and flexibility. Generally, there is a tradeoff between the probe size and spatial resolution. The transverse resolution of PAM can be determined by either light excitation or ultrasound detection, which correspond to optical- and acoustic-resolution PAM, respectively[55]. Optical-resolution PAM offers 1–2 orders of magnitude better transverse resolution but usually requires a more delicate optical design and thus has a larger footprint (>1 mm)[12,43,56–59]. This limits its application to larger internal organs with low tortuosity, such as the coronary artery and the gastrointestinal and vaginal tracts. Acoustic-resolution PAM with a relaxed requirement on light focusing is typically adopted for reduced probe size (<1 mm) to enable applications like imaging branches of the coronary artery[38,60,61]. However, the compromised transverse resolution (>100 μm) may lead to the miss of crucial pathological features such as the thin fibrous cap, a key precursor of plaque rupture[43,62]. Also, in both optical- and acoustic-resolution PAM, the axial resolution is limited by the bandwidth of ultrasound detection to tens or hundreds of microns[55], which prevents cellular-level imaging in 3D. The design and construction of endoscopic PAM probes have two major technical considerations, light delivery and ultrasound detection, both of which are crucial in determining the probe size and spatiotemporal resolution.

a. Light delivery

The light delivery approaches can be classified into three categories, distal scanning, proximal scanning, and full-field imaging, each of which has advantages and limitations in terms of the probe footprint, spatial resolution, and imaging speed.

1. Distal scanning (Fig. 2a): This approach involves the physical movement of either a portion or the entire endoscopic probe. For forward-viewing endoscopic PAM, miniaturized micro-electromechanical systems (MEMS) scanners are employed for 2D laser scanning over a field of view (FOV) of 10×10 mm^2 with a B-scan rate up to 500 Hz. However, the probe size is relatively large (11.5 mm)[53,59]. Such device can be useful for surgical guidance like tumor resection but is not small enough to image internal organs. Recently, a scanning fiber cantilever, previously introduced in multi-photon fluorescence endoscopy[63], was adopted for endoscopic PAM to achieve a reduced diameter of 3 mm (FOV: ~3 mm in diameter)[64]. In this design, the fiber tip is driven by a piezo actuator and moves along a spiral trajectory to achieve 2D scanning with a B-scan rate up to 130 Hz. For side-viewing endoscopic PAM[1,2], the most common design is to rotate either the internal optics or the entire probe to achieve B-scan at a rate up to 100 Hz[34]. Further, translating the probe along the axial direction allows the acquisition of multiple B-scans to form a 3D image. Requiring only 1D scan in the cross-sectional plane, the side-viewing endoscopic PAM has the advantage in probe size over the forward-viewing configuration and can be as small as 0.7 mm[38].
2. Proximal scanning (Fig. 2b): Unlike distal scanning that integrates a scanner inside the probe, proximal scanning uses light steering units in the remote interrogation system and thus enables a more compact design. This is particularly

beneficial for the forward-viewing configuration, which is more difficult to miniaturize. Fiber bundles or multi-core fibers, which have thousands of light-guiding cores distributed over the cross-section, have been adopted for proximal scanning in endoscopic PAM[58,65–67]. In this approach, the fiber's cross-section is projected onto the imaging plane via relay optics, enabling 2D scan by steering the laser beam into individual cores at the input end. The probe size is 2.4 mm with a FOV of >3.5 mm in diameter[58]. Although the reported A-line rate is only 1 kHz, it is possible to increase it to 1 MHz by using high-pulse-repetition-rate lasers[68]. A major drawback of this approach is the image pixelization and resolution impairment caused by gaps between the cores[69]. Recently, endoscopic imaging via a single multimode optical fiber (MMF) without additional optics has gained considerable interest, owing to the small footprint and free of image pixelization[70]. An endoscopic PAM probe with a diameter of 0.25 mm (FOV~ 0.1 mm in diameter) has been demonstrated by using a MMF[71]. In this approach, the transmission matrix of the MMF is measured to establish the relationship between the input and output fields[72–76], enabling 2D laser scanning through the modulation of the input field. This approach usually requires a delicate setup for measuring the complex optical field, and the A-line rate is limited by the refresh rate of the spatial light modulator (<47 kHz[72]). To simplify the design and enhance the speed, another approach is to use a set of speckle patterns from the MMF for illumination and perform imaging reconstruction by solving the inverse problem[71,77,78]. It has been shown that an image with 300×300 pixels can be formed through 4,096 patterns, resulting in an A-line rate of 483 kHz[71]. Despite the advantages of the MMF-based endoscopic PAM, its *in-vivo* performance and practical utility remain to be demonstrated (see additional discussions in Section IV).

3. Full-field imaging (Fig. 2c): In PAI, 3D imaging over the entire FOV can be achieved with a single, stationary laser pulse based on array-based ultrasound detection and tomographic image reconstruction[55]. The same principle has been adopted in endoscopic PAM[27,79–81], where an ultrasound array based on either piezoelectric transducers[27,80] or optical sensors[79,81] is used to detect the photoacoustic signals excited by an unfocused laser beam. This approach offers single-pulse 3D imaging and thus enhances imaging speed. However, the spatial resolution is limited by acoustic focusing, which is 1–2 orders of magnitude worse than the optically defined transverse resolution in the scanning-based PAM[55]. Also, the probe size is larger than 2 mm due to the need for an ultrasound array[82].

b. Ultrasound detection

1. Piezoelectric transducers (Fig. 2d): piezoelectric transducers are widely used for ultrasound detection in PAI, including endoscopic PAM[83]. Miniaturized piezoelectric transducers, including focused, un-focused, and transparent ones, have been adopted for endoscopic PAM[1]. Although focused ultrasound detection improves sensitivity, the limited aperture size in endoscopic PAM makes it difficult to achieve tight acoustic focus[84]. Thus, miniaturized unfocused transducers, which are easier to fabricate, are widely used in endoscopic PAM. To reduce the probe size, coaxial arrangement of the light delivery and ultrasound detection is desired. Although ring-shaped transducers offer a convenient means for such arrangement, the detection sensitivity is compromised because of the central opening[85]. As an alternative solution, transparent transducers have attracted increasing attention in endoscopic PAM[86]. However, a common limiting factor of piezoelectric transducers is that the sensitivity is proportional to the surface area. As a result, reducing the transducer size inevitably compromises the sensitivity if other factors (e.g., material and electrical circuit) remain unchanged[87].

2. Optical ultrasound sensors (Fig. 2e): Owing to the size-independent sensitivity, optical detection of ultrasonic waves has gained increasing attention[87]. It has been shown that optical ultrasound sensors offer a superior noise-equivalent pressure density over piezoelectric transducers when placed near the photoacoustic source[87], which well aligns with

the endoscopic application. Moreover, a detection bandwidth more than 200 MHz has been demonstrated[88], enhancing the axial resolution. Among various optical ultrasound sensors, including active fiber lasers[20] and passive microring[89] and Fabry–Pérot resonators[58,74,76,79,81], have shown great promise for endoscopic PAM. However, the optical resonator-based ultrasound detection has several limitations. First, the need for low-noise lasers and optoelectronics makes the interrogation system more complex than conventional transducers. Second, it is challenging to form an array of optical resonators for full-field imaging, due to the limited integrability and the low speed of interrogating multiple resonators concurrently[81,90]. Third, unlike piezoelectric transducers, existing optical ultrasound sensors can detect but not emit ultrasonic waves. This prevents the integration of endoscopic photoacoustic and ultrasound imaging, which has shown great promise in the detection of gastrointestinal cancer[11]. In addition, the robustness and stability of optical ultrasound detection *in vivo*, which is crucial for functional imaging, remains to be demonstrated (see additional discussion in Section III). More detailed information on optical ultrasound detection in PAM can be found in recent reviews[91,92].

3. Micromachined ultrasound transducers (MUT): Recent advances in the semiconductor and MEMS technologies have led to an emerging alternative to conventional ultrasound transducers: micromachined ultrasound transducer (MUT)[83]. Piezoelectric and capacitive MUTs (PMUT and CMUT, respectively) are the two primary types used in PAI. PMUTs incorporate a piezoelectric thin film clamped between two electrodes and mounted above a cavity. Unlike conventional transducers that operate in the thickness mode, PMUTs typically function in the flexural vibration mode, allowing for a reduction in the element thickness. However, PMUTs exhibit a relatively low electromechanical coupling coefficient (1–6%) compared to conventional piezoelectric transducers (~18%)[93]. In contrast, CMUTs have two parallel plates: a fixed bottom electrode and a suspended membrane with a top electrode. Ultrasonic waves impacting the top electrode induce vibrations in the membrane and alter the capacitance of the device, which is monitored over time for ultrasound detection. CMUTs demonstrate high electromechanical coupling coefficients (~70%) and sensitivity. However, they require high voltages (>80 V) to provide bias charges, posing a practical challenge for endoscopic applications[82,93].

Overall, MUTs have several advantages. Compared to conventional piezoelectric transducers, they offer reduced size and weight while maintaining relatively high sensitivity. Compared to optical ultrasound sensors, they offer the facile integration of a large number of elements and electrical interconnections to construct ultrasound arrays for full-field imaging[93,94]. A single-element size as small as 40 μm and a 103-element 2D array within a 2.5-mm-diameter footprint have been reported[95]. However, the detection bandwidth of existing MUTs is less than 20 MHz[82,95–99], which limits the axial resolution of endoscopic PAM. Moreover, similar to conventional piezoelectric transducers, the sensitivity of MUTs scales with its physical size, thus sharing similar limitations[93,100].

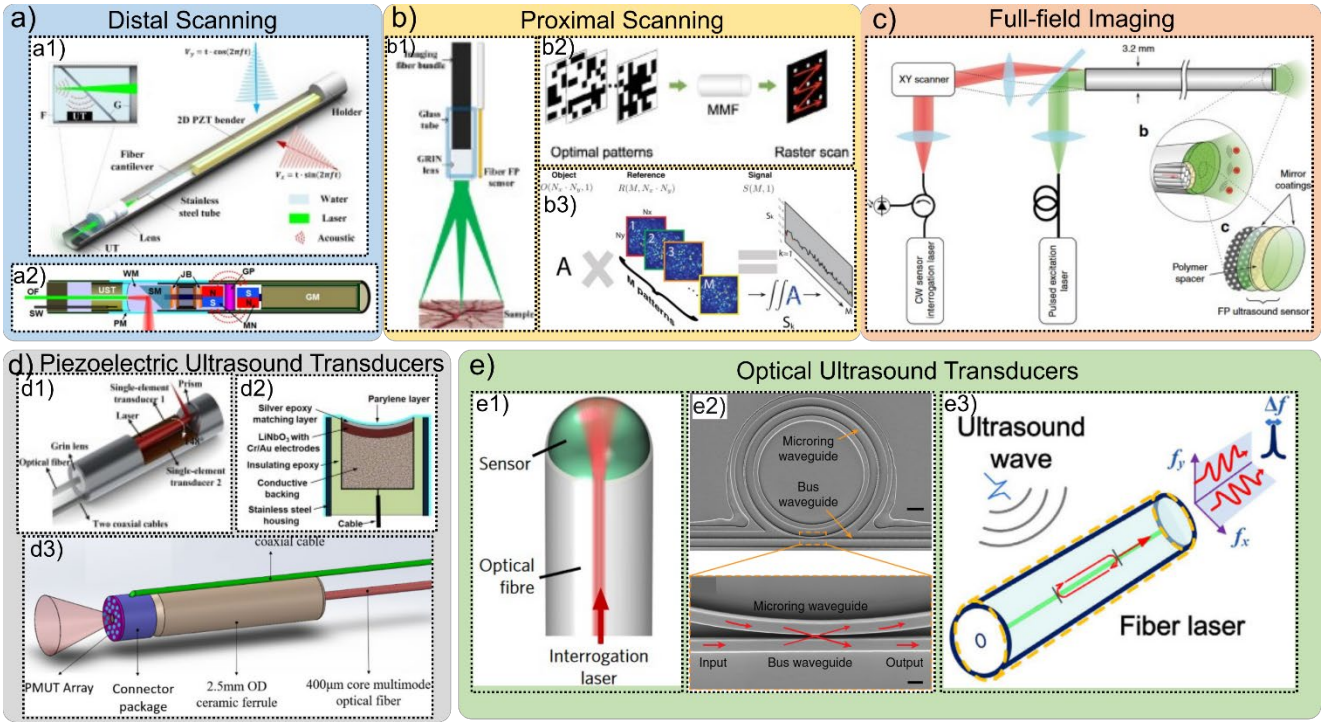

FIG. 2. Examples of the two key components in existing endoscopic PAM devices: light delivery (a)-(c) and ultrasound detection (d)-(e). (a) Distal scanning: a1) fiber catheter[64]; a2) rotor[101]. Reprinted with permission from [64] Copyright 2024 AIP Publishing. Reprinted with permission from [101] Copyright 2024 Optica Publishing Group. (b) Proximal scanning: b1) core-by-core scanning over a multi-core fiber[58]; b2) wavefront shaping[72]; b3) speckle illumination[71]. Reprinted with permission from [58] Copyright 2024 IEEE. Reprinted with permission from [72] Copyright 2024 Elsevier. Reprinted with permission from [71] Copyright 2024 AIP Publishing. (c) Full-field imaging based on an ultrasound array[81]. Reprinted with permission from [81] Copyright 2024 Springer Nature. (d) Piezoelectric ultrasound transducers: d1) unfocused transducer[42]; d2) focused transducer[102]; d3) PMUT transducer array[82]. Reprinted with permission from [42] Copyright 2024 Optica Publishing Group. Reprinted with permission from [82, 102] Copyright 2024 SPIE. (e) Optical ultrasound sensors: e1) fiber Fabry-Pérot sensor[103]; e2) microring resonator[104]; e3) fiber laser[105]. Reprinted with permission from [103-105] Copyright 2024 Springer Nature.

III. Challenges for endoscopic functional PAM

i. Functional imaging of the vasculature

A distinctive capability of PAI is label-free functional imaging of the vasculature, including blood oxygenation (sO_2) and flow. Based on these functional measurements, the oxygen extraction fraction (OEF) and metabolic rate of oxygen (MRO_2), which reflect tissue and organ viability, can be assessed[106]. Here, we discuss the technical requirements for quantifying each of these functional parameters and the corresponding challenges in the endoscopic setting.

a. Blood oxygenation

Reflecting blood oxygen supply, sO_2 is an important biomarker for detecting cancer and inflammation[20]. It can be quantified by measuring the concentrations of oxy- and deoxy-hemoglobin (HbO_2 and HbR, respectively), using either spectroscopic or nonlinear PAM. For the spectroscopic approach, the relative concentrations of HbO_2 and HbR are derived by performing least-squares fitting on the photoacoustic signals acquired at multiple optical wavelengths[107]. For accurate quantification of sO_2 using

this approach, the point spread functions at all wavelengths need to be identical. It has been shown that spatially mismatched multi-color light foci can cause significant errors in the sO_2 measurement[108]. To date, spectroscopic measurements for sO_2 have been achieved only in acoustic-resolution endoscopic PAM, where light is weakly focused[13,60,109,110], and only in gastrointestinal imaging, where the requirement of the probe size is relaxed[20]. In addition to the achromatic requirement, the signal-to-noise ratio (SNR) is another key factor. It has been shown that SNR plays a critical role in the sO_2 quantification[111]. When SNR is insufficient, noises measured at different wavelengths can be miscounted as 'fake' signals and affect the accuracy. Due to the lower collection efficiency of the photoacoustic signal in endoscopic PAM compared to the bench-top counterpart, higher laser fluence is often required to achieve a similar SNR (>40 mJ/cm^2 *vs.* <10 mJ/cm^2 for middle-size vessels with an average diameter of tens of micrometers)[13]. However, high laser fluence can induce nonlinear absorption due to the saturation effect and affect the accuracy of the spectroscopic measurement[112]. Also, there is no explicit guidance for the laser safety in internal organs[12]. Thus, it is desirable to use the minimum light dosage possible to avoid affecting normal physiology or causing tissue damage.

Nonlinear methods that capitalize on either intensity saturation[113] or variable pulse width[114] have also been developed for sO_2 quantification. These methods distinguish HbO_2 and HbR based on their saturation characteristics[112]. Specifically, the intensity saturation method exploits the nonlinear response of the photoacoustic signal to high pulse energy, whereas the variable pulse width technique relies on the differential responses of the photoacoustic signal to picosecond and nanosecond laser excitations. Notably, these nonlinear methods require only a single wavelength, simplifying the design and construction of the endoscopic probe by eliminating the need for achromatic components. However, the intensity saturation method requires relatively high pulse energy, which might cause safety concerns. The variable pulse width approach necessitates the use of a picosecond laser. In the context of endoscopic PAM, where optical fibers are commonly employed, transmitting picosecond pulses can lead to nonlinear effects, such as stimulated Raman scattering and four-wave mixing, within the fiber[115]. These effects may produce unwanted additional wavelengths and complicate sO_2 quantification[112].

b. Blood flow

Blood flow is another essential functional parameter of the vasculature[116]. PAM has demonstrated superb capability to measure blood flow owing to its high sensitivity to the optical absorption of red blood cells[106,117]; however, translating this measurement to the endoscopic setting faces challenges[118]. Various methods have been developed for blood flow measurements in PAM[106], where a common strategy is to extract the relation among the sequentially measured photoacoustic signals, such as the temporal correlation[119–121] and amplitude evolution[122,123]. Therefore, consistent and reliable measurements of photoacoustic signals over time are crucial for flow quantification, posing a challenge for endoscopic PAM. As discussed in the previous sections, current endoscopic PAM has a limited SNR especially for applications like intravascular imaging where the probe size is small. This constraint is expected to compromise the accuracy of flow measurements, as noise may confound the correlation analysis of photoacoustic signals. Optical ultrasound detectors, especially optical microresonators, hold great promise for endoscopic PAM of blood flow because their potential to achieve a high SNR with minimal physical size. However, there is a caveat. The optical microresonators are typically interrogated by tuning the wavelength of a narrow-bandwidth continuous-wave (CW) laser to the deflection point on the edge of the resonant peak/dip to maximize sensitivity[92]. Fluctuations in the ambient temperature can shift the resonant wavelength and induce a drift in the sensitivity of the microresonator at a fixed laser wavelength. For a decent polymer-based microresonator (SU8, $Q = 1\times10^5$, thermo-optic dependence: -95 pm/°C near 1550 nm)[124], as small as a 0.32-°C fluctuation can completely shift the resonant peak away from the intended interrogation wavelength and nullify its acoustic response. This issue may be exacerbated in the endoscopic setting because the sensor is placed inside living tissues that naturally

experience temperature fluctuations. Indeed, studies in different animal species have shown noticeable temperature fluctuations in the brain (±2–3 °C)[125]. Moreover, the close proximity of the endoscopic probe to the photoacoustic source can lead to rapid temperature changes due to light absorption, especially when a high-repetition-rate laser is used for high-speed imaging[126]. In addition, strains imposed on the microresonator due to its physical contact with local tissues can also shift in the resonant peak. These fluctuations in the sensitivity of optical ultrasound sensors may affect the correlation analysis of sequentially measured photoacoustic signals for blood flow quantification.

c. Oxygen extraction fraction and metabolic rate of oxygen

Derived from sO_2, OEF is a critical parameter that reflects tissue's ability to extract oxygen from the blood stream to maintain functional and morphological integrity[127]. It is indicative of oxygen utilization efficiency in the tissue and serves as an important biomarker in cancer[128] and ischemia[129]. Additionally, MRO_2, which can be derived from blood flow and OEF, provides a direct measure of tissue's oxygen consumption and can be used for monitoring tissue viability and assessing treatment responses[106]. Therefore, the accuracy of sO_2 and blood flow measurements by endoscopic functional PAM determines its capability for the quantification of OEF and MRO_2.

ii. Multi-contrast imaging

Co-registered, multi-contrast imaging provides a more comprehensive assessment of the tissue, holding great promise in areas such as intraoperative tumor detection for surgery guidance[128]. Combining the abundant contrasts of endogenous chromophores (Fig. 1a) and exogenous contrast agents[130–132] with the excellent multiplexing capability of light, PAM is well suited for multi-contrast imaging. Indeed, benchtop PAM has demonstrated simultaneous imaging of the tumor vasculature and tumor-contrast-enhancing agents using visible and near-infrared excitations[128]. However, achieving multi-contrast imaging in endoscopic PAM faces a significant challenge: the device needs to operate in a wide spectral range with minimal chromatic dispersion[128]. Despite the broad transparent window (200-2400 nm), fused silica fibers (i.e., step-index or graded-index fibers), which is widely used in endoscopic PAM, are subject to pronounced chromatic dispersion[133]. Single-mode fibers, which are required for tight light focusing, can only operate within a wavelength range of a few hundred nanometers without becoming few-mode or lossy[133]. In addition, conventional designs of an apochromatic optical system require multiple optical elements[134], posing challenges for miniaturization into an endoscopic device. Moreover, GRIN lens, which is widely used in endoscopic PAM to achieve strong light focusing, exhibits strong chromatic and spherical aberration[135]. As a result, most existing endoscopic PAM devices are only capable of providing a single contrast.

Table I summarizes the challenges for endoscopic PAM to achieve functional and multi-contrast imaging. There are three main considerations for addressing these unmet challenges, including (1) compact, achromatic, and aberration-free light delivery; (2) sufficient SNR for accurate functional measurements at low-light conditions with minimum physiological perturbation; and (3) miniature, high-sensitivity, and stable ultrasound detection. In the following section, we highlight recent technical advances in five areas that, in our perspective, hold the potential to address the current limitations of endoscopic PAM towards functional imaging. Table 1 also summarizes how the five areas can facilitate specific functional measurements.

TABLE I. Challenges and strategies towards endoscopic functional PAM

Parameters	Methods	Requirements	Challenges	Strategies
sO_2, OEF, and MRO_2	Multi-wavelength spectroscopic method	• Low chromatic aberration • High SNR	• Bulky optical elements for achromatic design • High-sensitivity, robust ultrasound detection	• 3D printed micro-optics • Wavefront shaping • Robust optical sensing of ultrasound • Computational approaches
	Single-wavelength nonlinear methods	• Transmit picosecond pulse	• Optical nonlinearity in fiber	• Microstructured fiber
Blood flow and MRO_2	Temporal correlation or amplitude evolution	• High SNR • Stable ultrasound detection	• High-sensitivity, robust ultrasound detection	• Robust optical ultrasound sensing • Computational approaches
Multi-contrast	Multi-spectral excitation	• Broadband light delivery • Low chromatic aberration	• Chromatic dispersion in fiber • Limited spectral range for single-mode operation in fiber • Bulky optical elements for apochromatic design	• Microstructured fiber • 3D printed micro-optics

IV. Strategies towards endoscopic functional PAM

i. Microstructured optical fibers

Microstructured optical fibers are distinguished by their ability to tailor light propagation properties, such as dispersion, modal profile, and nonlinearity[136]. Although their use in endoscopic PAM remains largely unexplored, these fibers have shown great promise in multi-photon endoscopy by reducing nonlinear pulse broadening[137–139]. Specifically, endless-single-mode photonic crystal fibers (PCFs), capable of maintaining single-mode operation across a wide spectral range from visible to near-infrared, are well suited for multi-contrast imaging where consistent performance over varying wavelengths is crucial[140]. Moreover, both large-mode-area[141] and hollow-core PCFs[142–144] significantly reduce the optical nonlinearity. This is particularly important for enhancing the accuracy of sO_2 quantification using nonlinear methods, where ultrashort laser pulses are used and nonlinearity-induced pulse distortions could compromise the measurement accuracy. The adaptation of the various PCFs, which are broadly available, in endoscopic PAM is expected to help address current challenges in sO_2 measurements and multi-contrast imaging.

ii. 3D printed micro-optics

Recent emergence of ultrafast laser-based 3D printing, also known as two-photon polymerization and laser direct writing, has revolutionized the fabrication of micro-optical elements, stacked components, and integrated devices[145]. In-depth reviews on this topic are available[146–148]. In this technique, ultrafast laser pulses (typically 100–300 fs) are used to selectively irradiate a photosensitive material, resulting in the removal or retention of the laser-irradiated region after post-chemical processing to form desired 3D microstructures[148]. By shaping the light field into any desired geometry, such as point-to-point scanning[149] or patterned illumination[150], this method enables 3D freeform fabrication on various substrates, including optical fibers (Fig. 3a-b). Ultrafast laser 3D print has been applied to fabricate micro-lenses[151–154] and diffractive micro-optics[155–159], showing promise in mitigating the aberration issues associated with existing off-the-shelf micro-optics such as ball or GRIN lenses. Moreover, laser 3D printing of achromatic optics has been reported[160–162], potentially benefiting endoscopic PAM-based sO_2 and multi-contrast imaging that use multiple excitation wavelengths. Going beyond proof-of-concept, 3D printed micro-optics have been

used by other modalities, including OCT and fluorescence imaging, for endoscopic applications *in vivo* [163–165]. Thus, ultrafast laser 3D printing presents a promising solution for compact, achromatic, and aberration-free light delivery in endoscopic PAM.

iii. Wavefront shaping

Compact light delivery can also be achieved by controlling the output light field of a MMF through wavefront shaping[70,166]. Here, we focus on the specific aspects of wavefront shaping that are relevant to endoscopic PAM. There are two advantages of using wavefront shaping for endoscopic imaging. First, it eliminates the need for additional optics in the probe construction, resulting in a reduced footprint and simplified fabrication. Second, it enables the generation of arbitrary light fields without modifying the probe design, enhancing the imaging capability. For example, axial scanning can be achieved by modulating the wavefront to focus at different depths[167]. Typically, the wavefront shaping is performed by a phase-only liquid-crystal spatial light modulator (LC-SLM), due to the high modulation efficiency[168]. However, the low frame rate (<1 kHz) of existing LC-SLMs limits the image speed (<0.5 Hz for an image containing 2,500 pixels) and is insufficient for the dense spatial sampling required by certain functional measurements, such as the correlation-based blood flow quantification[169,170]. Recent applications of the Lee-hologram[171] or real-valued intensity transmission matrix[172] have enabled the use of high-speed intensity modulators, such as the digital micromirror device (DMD; >30 kHz frame rate), to overcome this limitation. Using this approach, forward-view endoscopic PAM with a speed as high as 57 frames/second has been demonstrated[72–74]. Even faster modulation has been achieved using a 1D modulator with a 350-kHz frame rate and 1D-to-2D transform[173], but its applicability in MMF imaging is yet to be explored. DMD can also produce a high power ratio (the ratio between the power carried by the primary light focus at the distal end of the MMF and the total power exiting the MMF) up to 75%[168], which can boost the image contrast. Despite the promise, wide adoption of wavefront shaping for *in-vivo* endoscopic imaging still faces a major challenge—the transmission matrix of a MMF is highly sensitive to perturbations, such as fiber bending, twisting, and temperature fluctuations[70]. Deriving the transmission matrix typically requires access to both ends of the fiber, which is largely impractical *in vivo*. The challenge is exacerbated in intravascular and gastrovascular imaging, where the probe is maneuvered inside a tortuous structure and its shape changes constantly. Several approaches have been developed for single-end calibration[174–179]. In particular, an adaptive tracking method based on a pre-calculated database and dimension reduction allows recalibration of the transmission matrix at a 1 kHz with single-end access, enabling endoscopic fluorescence imaging in live mice[178]. Another approach to achieve stable light field propagation through the MMF is to intentionally introduce random fluctuations of the refractive index in the fiber, leading to field localization in the transversal plane during light progopation[180]. The disordered optical fibers have been shown to facilitate image transfer with low cross-talk[181–184]; however, the *in-vivo* performance remains to be tested. With advances in fast wavefront modulation, single-end calibration, and specially designed optical fibers, wavefront shaping is expected to play an increasingly significant role in endoscopic PAM.

iv. Robust optical sensing of ultrasound

Although optical microresonator-based ultrasound sensors hold great potential in endoscopic PAM, their practical usage has been hindered by issues in reliability and stability. One solution is to actively tune the laser wavelength to the sensor's resonance through the Pound-Drever-Hall (PDH) frequency-locking technique[185]. In this approach, the phase of the interrogation laser is modulated to introduce an interference between the carrier and sideband with a frequency identical to the frequency difference between the laser and the microresonator's resonance, from which a PDH error signal can be derived. By minimizing this error,

the laser frequency can be locked to the resonant peak. However, further development is needed to extend the dynamic range for *in-vivo* applications[186]. Alternatively, methods based on broadband interrogation have been developed to resolve the entire resonant peak, which do not require spectral overlap between the laser and the microresonator's resonance and therefore are insensitive to the drift of the resonant wavelength[90,186–188]. In this approach, high-repetition-rate laser pulses are used to generate a coherent broadband source (i.e., frequency comb), whose spectral envelope is modulated by the microresonator's resonance. An interferometer is then used to extract the mean shift of the resonance for deriving the photoacoustic signal. Although this approach is more complex because of the need for pulse interferometry, recent advances in integrated photonics, such as on-chip frequency comb and photonic circuits, may simplify the system and facilitate its adoption in PAM[189]. Compared to passive microresonators, active microresonators (e.g., lasing cavity) may exhibit a better sensing stability. Fiber-laser-based ultrasound sensors, which detect the beating between two orthogonally polarized lasing modes induced by the acoustic-pressure-generated birefringence, have been applied in endoscopic PAM[20,105]. Primarily sensitive to asymmetric perturbations, this technique, in principle, is less susceptive to ambient temperature fluctuations[190]. Overall, future efforts should focus on the development of robust and effective interrogation schemes to facilitate the practical usage of optical ultrasound sensors in endoscopic PAM.

Another promising strategy for endoscopic PAM is non-contact optical detection of ultrasound, where the photoacoustic signal is derived by extracting its modulation of the local optical phase[191,192] or reflectance[193,194]. In this approach, a CW laser is used to probe the phase or intensity modulation induced by the photoacoustic pressure. Compared to phase modulation, reflectance-intensity modulation is less susceptive to the background oscillations of the tissue and has enabled *in-vivo* imaging of the mouse ear microvasculature with an SNR comparable to bench-top PAM using a piezoelectric transducer[194]. This approach holds great promise for endoscopic PAM because it eliminates the need for an ultrasound sensor, allowing the delivery of both the pulsed photoacoustic excitation light and the CW interrogation light through the same fiber. This greatly simplifies the probe design and reduces its size[195]. Moreover, since no acoustic coupling is required, the endoscopic probe can be physically isolated from the targeted tissues and hosed inside a biocompatible housing. This not only minimizes the risk of infection but also broadens the range of material options for the design.

v. Computational approaches

In addition to advancing the device itself, computational methods can be highly complementary for enhancing the performance of endoscopic PAM. Specifically, machine learning has shown considerable promise in improving the SNR[111,196–198]. Recently, a two-step sparse coding-based method was developed to denoise images acquired with low-fluence bench-top PAM, leading to significant improvements in microvascular visualization and quantitative accuracy of sO_2 and blood flow measurements[111]. This method capitalizes on the fact that unfeatured noise patterns have less correlation and sparsity compared to photoacoustic signals, allowing them to be separated using sparse coding. The results show that at one-fifth of the normal laser fluence, this approach reduces the errors in functional measurements of microvascular sO_2 and flow from 20% to less than 5%. Overall, the development of computational methods for post-processing can enhance image quality, thereby relaxing requirements on the device and serving as a parallel direction to realize the potential of endoscopic PAM for functional imaging.

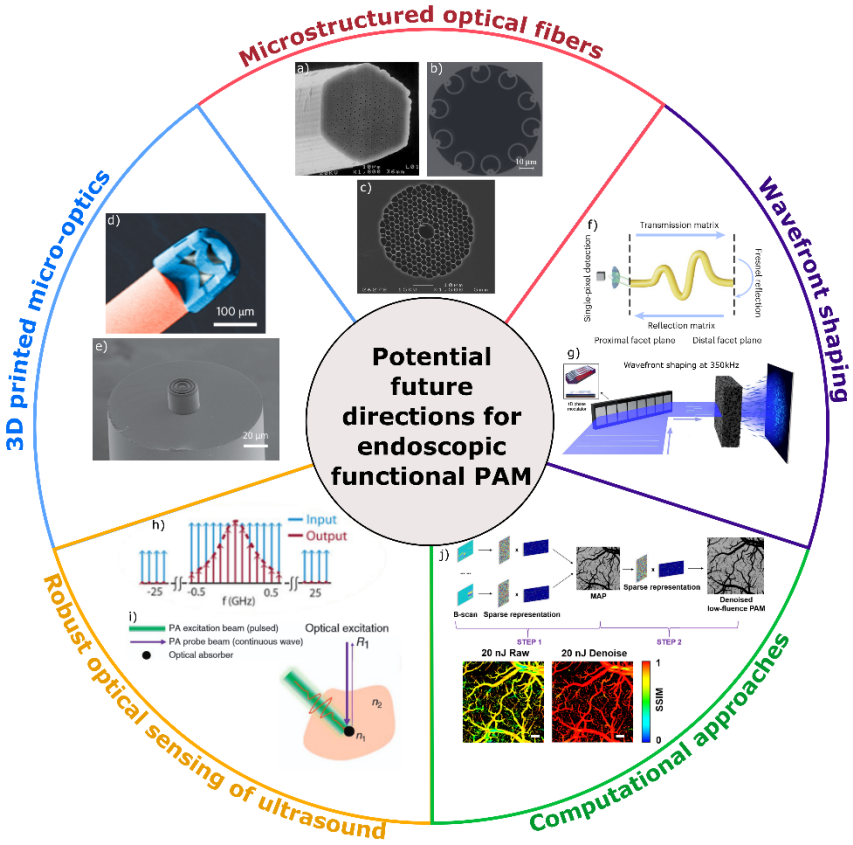

FIG. 3. Potential future directions for endoscopic functional PAM. Microstructured optical fibers: a) endless-single-mode photonic crystal fibers[140]; b) anti-resonant hollow-core fibers[199]; c) hollow-core photonic crystal fibers[144]. Reprinted with permission from [140] Copyright 2024 Optica Publishing Group. Reprinted with permission from [199] Copyright 2024 IOP Publishing. Reprinted with permission from [144] Copyright 2024 Optica Publishing Group. 3D printed micro-optics on the fiber tip: d) multi-element micro-objective lens[154]; e) inverse-designed metalens[159]. Reprinted with permission from [154] Copyright 2024 Springer Nature. Reprinted with permission from [159] Copyright 2024 American Chemical Society. Robust, fast wavefront shaping: f) measurement of the transmission matrix of a multi-mode fiber at 1 kHz using single-end access and dimension-reduction strategy[178]; g) wavefront shaping with a 1D spatial light modulator and 1D-2D transform at 350 kHz[173]. Reprinted with permission from [178] Copyright 2024 Springer Nature. Reprinted with permission from [173] Copyright 2024 Springer Nature. Optical photoacoustic detection: h) resolving the entire resonant peak of an optical micro-resonator with pulse interferometry[187]; i) non-contact detection of initial photoacoustic pressure with light[200]. Reprinted with permission from [187] Copyright 2024 Wiley. Reprinted with permission from [200] Copyright 2024 Springer Nature. Computational imaging: j) two-step sparse coding-based denoising to improve image quality and quantitative accuracy in low-fluence benchtop PAM[111]. SSIM: structural Similarity Index Measure. Scale bar: 200 µm. Reprinted with permission from [111] Copyright 2024 IEEE.

V. Emerging opportunities for endoscopic functional PAM

Future advances in endoscopic PAM to enable functional imaging and further miniaturization will not only enhance its efficacy in existing applications but also open additional avenues in both clinical research and basic science.

On the clinical front, a promising application lies in intravascular imaging of cerebral arteries. Endovascular interventions have become increasingly important for treating cerebrovascular conditions such as aneurysm, ischemic occlusion, and intracranial atherosclerotic disease[201,202]. Accurate diagnosis of intracranial artery pathology and identification of perioperative events are crucial for effective treatment, propelling the growing interest in intravascular imaging in the brain[203,204]. However, challenges persist due to the small diameter and high tortuosity of cerebral vessels, necessitating highly flexible probes with minimal size. Endoscopic OCT with a probe size as small as 0.4 mm is suitable for this purpose, but only allows structural imaging[205,206]. By providing functional insights, endoscopic PAM has the potential to advance the diagnosis and management of cerebrovascular disease. Another promising area is intrathecal spinal cord imaging. Pathologies affecting the spinal cord, such as trauma, tumors, and infections, exhibit distinct hemodynamic and metabolic characteristics[207]. However, imaging the spinal cord is challenging due to the surrounding bony anatomy and limited space. Non-invasive modalities, such as CT, MRI, and US, suffer from limited spatial resolution[208,209]. Surgical exposure, while providing access, is too invasive for diagnostic purposes[210,211]. Achieving high resolution in a minimally invasive manner, endoscopy is preferable. To minimize lumbar drains, the probe diameter should be less than 1 mm[212,213]. A recent study using a 0.9-mm endovascular OCT probe reported high-resolution, artifact-free structural imaging of epidural veins, pial lining, and nerve rootlets[213], showcasing the promise of endoscopic imaging of the spinal cord. By adding functional contrasts, endoscopic PAM is poised to better assist clinicians in identifying pathologies, guiding surgical procedures, and assessing treatment outcomes.

In basic research using animal models, endoscopic PAM can help advance our understanding of microvascular physiology and pathology in deep brain. Cerebral microvascular dysfunction has been linked to neurodegeneration, such as that in Alzheimer's disease, which often begins in deep-brain regions (e.g., hippocampus)[214,215]. Understanding microvascular impairments in the early stage of neurodegeneration may reveal additional insights into pathogenesis and promote early detection or treatment. Benchtop PAM, although enabling comprehensive assessment of microvascular function and tissue oxygen metabolism, cannot penetrate the superficial cortex[216]. Endoscopic implementation is thus needed to extend the success of PAM in functional microvascular imaging to deep brain. Another potential application lies in intravital imaging of the beating heart. Microcirculatory dysfunction in cardiovascular disease can result in fatal outcomes, such as septic shock and heart failure, irrespective of alterations in the broader systemic circulation[217]. *In-vivo* functional imaging of the heart microvasculature can reveal the much needed insights into the underlying disease mechanisms, but it is difficult to access due to the ribs and lungs surrounding the heart[218]. Although non-invasive modalities[218] and open-chest procedures[219] have been explored, they either cannot provide sufficient resolution to image the microvasculature or cause significant perturbations to heart physiology. Advances in fluorescence micro-endoscopy, by inserting a 1.25-mm-diameter probe through the rib cage, have enabled intravital imaging of the beating heart with minimum disturbance to normal physiology, reduced motion artifacts, and longitudinal access[220,221]. Following this approach, endoscopic PAM holds the potential to further advance cardiovascular research by providing extra functional insights into the heart.

VI. Conclusion

In this Perspective, we have assessed the current state of endoscopic PAM, with a particular emphasis on its functional imaging capability. We have identified critical gaps to be addressed, including the need for miniaturized and achromatic light delivery, robust, compact, and high-sensitivity ultrasound detectors, and improved SNR to reduce light exposure and ensure quantitative

accuracy. Also, we have highlighted recent advances in microstructured optical fibers, ultrafast laser 3D printing, wavefront shaping, optical sensing of ultrasound, and computational imaging, which hold significant promise for addressing the existing challenges in endoscopic functional PAM and are poised to shape the future of this rapidly evolving field. In addition, we have suggested future opportunities for functional endoscopic PAM in both clinical applications and basic science research.

Acknowledgments

The authors appreciate the supports from the National Institutes of Health (NS120481, AG079503, NS125677, AT012283, and AG07772001), National Science Foundation (NSF CAREER 202988), and McDonnell Center of Systems Neuroscience Small Grants Program (FY24).

References

[1] Y. Li, G. Lu, Q. Zhou, and Z. Chen, "Advances in Endoscopic Photoacoustic Imaging," Photonics **8**(7), 281 (2021).

[2] H. Guo, Y. Li, W. Qi, and L. Xi, "Photoacoustic endoscopy: A progress review," Journal of Biophotonics **13**(12), e202000217 (2020).

[3] R. Banerjee, and D.N. Reddy, "Advances in endoscopic imaging: Advantages and limitations," Journal of Digestive Endoscopy **03**(S 5), 7–12 (2012).

[4] T. Rösch, "Endoscopic ultrasonography: imaging and beyond," Gut **52**(8), 1220–1226 (2003).

[5] M.J. Gora, M.J. Suter, G.J. Tearney, and X. Li, "Endoscopic optical coherence tomography: technologies and clinical applications [Invited]," Biomed. Opt. Express, BOE **8**(5), 2405–2444 (2017).

[6] V. Kučikas, M.P. Werner, T. Schmitz-Rode, F. Louradour, and M.A.M.J. van Zandvoort, "Two-Photon Endoscopy: State of the Art and Perspectives," Mol Imaging Biol **25**(1), 3–17 (2023).

[7] V.G. Andreev, A.A. Karabutov, and A.A. Oraevsky, "Detection of ultrawide-band ultrasound pulses in optoacoustic tomography," IEEE Transactions on Ultrasonics, Ferroelectrics, and Frequency Control **50**(10), 1383–1390 (2003).

[8] I.G. Calasso, W. Craig, and G.J. Diebold, "Photoacoustic Point Source," Phys. Rev. Lett. **86**(16), 3550–3553 (2001).

[9] J. Yao, and L.V. Wang, "Photoacoustic microscopy," Laser & Photonics Reviews **7**(5), 758–778 (2013).

[10] T. Zhao, A.E. Desjardins, S. Ourselin, T. Vercauteren, and W. Xia, "Minimally invasive photoacoustic imaging: Current status and future perspectives," Photoacoustics **16**, 100146 (2019).

[11] K. Zhang, J. Qiu, F. Yang, J. Wang, X. Zhao, Z. Wei, N. Ge, Y. Chen, and S. Sun, "Photoacoustic endoscopy and EUS: Shaking the future of multimodal endoscopy," Endoscopic Ultrasound **11**(1), 1 (2022).

[12] J.-M. Yang, C. Li, R. Chen, B. Rao, J. Yao, C.-H. Yeh, A. Danielli, K. Maslov, Q. Zhou, K.K. Shung, and L.V. Wang, "Optical-resolution photoacoustic endomicroscopy in vivo," Biomed. Opt. Express, BOE **6**(3), 918–932 (2015).

[13] J.-M. Yang, C. Favazza, R. Chen, J. Yao, X. Cai, K. Maslov, Q. Zhou, K.K. Shung, and L.V. Wang, "Simultaneous functional photoacoustic and ultrasonic endoscopy of internal organs in vivo," Nat Med **18**(8), 1297–1302 (2012).

[14] A. Horiguchi, M. Shinchi, A. Nakamura, T. Wada, K. Ito, T. Asano, H. Shinmoto, H. Tsuda, and M. Ishihara, "Pilot Study of Prostate Cancer Angiogenesis Imaging Using a Photoacoustic Imaging System," Urology **108**, 212–219 (2017).

[15] M. Wu, G. Springeling, M. Lovrak, F. Mastik, S. Iskander-Rizk, T. Wang, H.M.M. van Beusekom, A.F.W. van der Steen, and G.V. Soest, "Real-time volumetric lipid imaging in vivo by intravascular photoacoustics at 20 frames per second," Biomed. Opt. Express, BOE **8**(2), 943–953 (2017).

[16] Y. Qu, C. Li, J. Shi, R. Chen, S. Xu, H. Rafsanjani, K. Maslov, H. Krigman, L. Garvey, P. Hu, P. Zhao, K. Meyers, E. Diveley, S. Pizzella, L. Muench, N. Punyamurthy, N. Goldstein, O. Onwumere, M. Alisio, K. Meyenburg, J. Maynard, K. Helm, J. Slaughter, S. Barber, T. Burger, C. Kramer, J. Chubiz, M. Anderson, R. McCarthy, S.K. England, G.A. Macones, Q. Zhou, K.K. Shung, J. Zou, M.J. Stout, M. Tuuli, and L.V. Wang, "Transvaginal fast-scanning optical-resolution photoacoustic endoscopy," JBO **23**(12), 121617 (2018).

[17] R. Lin, S. Lv, W. Lou, X. Wang, Z. Xie, S. Zeng, R. Chen, W. Gao, T. Jiang, K.-W.E. Cheng, K.-H. Lam, and X. Gong, "In-vivo assessment of a rat rectal tumor using optical-resolution photoacoustic endoscopy," Biomed. Opt. Express, BOE **15**(4), 2251–2261 (2024).

[18] H. He, L. Englert, and V. Ntziachristos, "Optoacoustic Endoscopy of the Gastrointestinal Tract," ACS Photonics **10**(3), 559–570 (2023).

[19] Y. Zhu, L. Ni, G. Hu, L.A. Johnson, K.A. Eaton, X. Wang, P.D.R. Higgins, and G. Xu, "Prototype endoscopic photoacoustic-ultrasound balloon catheter for characterizing intestinal obstruction," Biomed. Opt. Express, BOE **13**(6), 3355–3365 (2022).

[20] Y. Liang, W. Fu, Q. Li, X. Chen, H. Sun, L. Wang, L. Jin, W. Huang, and B.-O. Guan, "Optical-resolution functional gastrointestinal photoacoustic endoscopy based on optical heterodyne detection of ultrasound," Nat Commun **13**(1), 7604 (2022).

[21] Z. Ali, C. Zakian, Q. Li, J. Gloriod, S. Crozat, F. Bouvet, G. Pierre, V. Sarantos, M. Di Pietro, K. Flisikowski, P. Andersen, W. Drexler, and V. Ntziachristos, "360º optoacoustic capsule endoscopy at 50 Hz for esophageal imaging," Photoacoustics **25**, 100333 (2022).

[22] X. Li, K. Xiong, and S. Yang, "Large-depth-of-field optical-resolution colorectal photoacoustic endoscope," Applied Physics Letters **114**(16), 163703 (2019).

[23] H. Lei, L.A. Johnson, K.A. Eaton, S. Liu, J. Ni, X. Wang, P.D.R. Higgins, and G. Xu, "Characterizing intestinal strictures of Crohn's disease in vivo by endoscopic photoacoustic imaging," Biomed. Opt. Express, BOE **10**(5), 2542–2555 (2019).

[24] H. He, A. Stylogiannis, P. Afshari, T. Wiedemann, K. Steiger, A. Buehler, C. Zakian, and V. Ntziachristos, "Capsule optoacoustic endoscopy for esophageal imaging," Journal of Biophotonics **12**(10), e201800439 (2019).

[25] D. Jin, F. Yang, Z. Chen, S. Yang, and D. Xing, "Biomechanical and morphological multi-parameter photoacoustic endoscope for identification of early esophageal disease," Applied Physics Letters **111**(10), 103703 (2017).

[26] J.M. Yang, C. Favazza, J. Yao, R. Chen, Q. Zhou, K.K. Shung, and L.V. Wang, "Three-Dimensional Photoacoustic Endoscopic Imaging of the Rabbit Esophagus," PLOS ONE **10**(4), e0120269 (2015).

[27] Y. Yuan, S. Yang, and D. Xing, "Preclinical photoacoustic imaging endoscope based on acousto-optic coaxial system using ring transducer array," Opt. Lett., OL **35**(13), 2266–2268 (2010).

[28] J. Jiang, C. Yuan, J. Zhang, Z. Xie, and J. Xiao, "Spectroscopic photoacoustic/ultrasound/optical-microscopic multimodal intrarectal endoscopy for detection of centimeter-scale deep lesions," Front. Bioeng. Biotechnol. **11**, (2023).

[29] X. Leng, K.M.S. Uddin, W. Chapman, H. Luo, S. Kou, E. Amidi, G. Yang, D. Chatterjee, A. Shetty, S. Hunt, M. Mutch, and Q. Zhu, "Assessing Rectal Cancer Treatment Response Using Coregistered Endorectal Photoacoustic and US Imaging Paired with Deep Learning," Radiology **299**(2), 349–358 (2021).

[30] Y. Yuan, G. Zhang, Y. Chen, H. Ni, M. Li, M. Sturek, and J.-X. Cheng, "A high-sensitivity high-resolution intravascular photoacoustic catheter through mode cleaning in a graded-index fiber," Photoacoustics **29**, 100451 (2023).

[31] R. Lin, Q. Zhang, S. Lv, J. Zhang, X. Wang, D. Shi, X. Gong, and K. Lam, "Miniature intravascular photoacoustic endoscopy with coaxial excitation and detection," Journal of Biophotonics **16**(4), e202200269 (2023).

[32] K. Zhan, L. Wang, Z. Chen, and D. Xing, "Intravascular Photoacoustic and Autofluorescence Imaging for Detecting Intraplaque Hemorrhage: A Feasibility Study," IEEE Journal of Selected Topics in Quantum Electronics **27**(4), 1–5 (2021).

[33] J. Leng, J. Zhang, C. Li, C. Shu, B. Wang, R. Lin, Y. Liang, K. Wang, L. Shen, K. Lam, Z. Xie, X. Gong, J. Ge, and L. Song, "Multi-spectral intravascular photoacoustic/ultrasound/optical coherence tomography tri-modality system with a fully-integrated 0.9-mm full field-of-view catheter for plaque vulnerability imaging," Biomed. Opt. Express, BOE **12**(4), 1934–1946 (2021).

[34] Z. Xie, C. Shu, D. Yang, H. Chen, C. Chen, G. Dai, K.H. Lam, J. Zhang, X. Wang, Z. Sheng, D. Gao, C. Liu, L. Song, and X. Gong, "In vivo intravascular photoacoustic imaging at a high speed of 100 frames per second," Biomed. Opt. Express, BOE **11**(11), 6721–6731 (2020).

[35] X. Wen, P. Lei, K. Xiong, P. Zhang, and S. Yang, "High-robustness intravascular photoacoustic endoscope with a hermetically sealed opto-sono capsule," Opt. Express, OE **28**(13), 19255–19269 (2020).

[36] Y. Cao, M. Alloosh, M. Sturek, and J.-X. Cheng, "Highly sensitive lipid detection and localization in atherosclerotic plaque with a dual-frequency intravascular photoacoustic/ultrasound catheter," Translational Biophotonics **2**(3), e202000004 (2020).

[37] L. Wang, P. Lei, X. Wen, P. Zhang, and S. Yang, "Tapered fiber-based intravascular photoacoustic endoscopy for high-resolution and deep-penetration imaging of lipid-rich plaque," Opt. Express, OE **27**(9), 12832–12840 (2019).

[38] P. Lei, X. Wen, L. Wang, P. Zhang, and S. Yang, "Ultrafine intravascular photoacoustic endoscope with a 0.7 mm diameter probe," Opt. Lett., OL **44**(22), 5406–5409 (2019).

[39] P. Wang, Z. Chen, F. Yang, S. Yang, and D. Xing, "Intravascular tri-modality system: Combined ultrasound, photoacoustic, and elasticity imaging," Applied Physics Letters **113**(25), 253701 (2018).

[40] S.J. Mathews, C. Little, C.D. Loder, R.D. Rakhit, W. Xia, E.Z. Zhang, P.C. Beard, M.C. Finlay, and A.E. Desjardins, "All-optical dual photoacoustic and optical coherence tomography intravascular probe," Photoacoustics **11**, 65–70 (2018).

[41] Z. Piao, T. Ma, J. Li, M.T. Wiedmann, S. Huang, M. Yu, K. Kirk Shung, Q. Zhou, C.-S. Kim, and Z. Chen, "High speed intravascular photoacoustic imaging with fast optical parametric oscillator laser at 1.7 μm," Applied Physics Letters **107**(8), 083701 (2015).

[42] X. Ji, K. Xiong, S. Yang, and D. Xing, "Intravascular confocal photoacoustic endoscope with dual-element ultrasonic transducer," Opt. Express, OE **23**(7), 9130–9136 (2015).

[43] X. Bai, X. Gong, W. Hau, R. Lin, J. Zheng, C. Liu, C. Zeng, X. Zou, H. Zheng, and L. Song, "Intravascular Optical-Resolution Photoacoustic Tomography with a 1.1 mm Diameter Catheter," PLOS ONE **9**(3), e92463 (2014).

[44] B. Wang, A. Karpiouk, D. Yeager, J. Amirian, S. Litovsky, R. Smalling, and S. Emelianov, "Intravascular photoacoustic imaging of lipid in atherosclerotic plaques in the presence of luminal blood," Opt. Lett., OL **37**(7), 1244–1246 (2012).

[45] A. Wiacek, K.C. Wang, H. Wu, and M.A.L. Bell, "Photoacoustic-Guided Laparoscopic and Open Hysterectomy Procedures Demonstrated With Human Cadavers," IEEE Transactions on Medical Imaging **40**(12), 3279–3292 (2021).

[46] C. Miranda, J. Barkley, and B.S. Smith, "Intrauterine photoacoustic and ultrasound imaging probe," JBO **23**(4), 046008 (2018).

[47] A. Horiguchi, K. Tsujita, K. Irisawa, T. Kasamatsu, K. Hirota, M. Kawaguchi, M. Shinchi, K. Ito, T. Asano, H. Shinmoto, H. Tsuda, and M. Ishihara, "A pilot study of photoacoustic imaging system for improved real-time visualization of neurovascular bundle during radical prostatectomy," The Prostate **76**(3), 307–315 (2016).

[48] H.S. Salehi, P.D. Kumavor, H. Li, U. Alqasemi, T. Wang, C. Xu, and Q. Zhu, "Design of optimal light delivery system for co-registered transvaginal ultrasound and photoacoustic imaging of ovarian tissue," Photoacoustics **3**(3), 114–122 (2015).

[49] M. Basij, Y. Yan, S. Alshahrani, I. Winer, J. Burmeister, M. Dominello, and M. Mehrmohammadi, "Development of an Ultrasound and Photoacoustic Endoscopy System for Imaging of Gynecological Disorders," in *2018 IEEE International Ultrasonics Symposium (IUS)*, (2018), pp. 1–4.

[50] S. Nandy, A. Mostafa, I.S. Hagemann, M.A. Powell, E. Amidi, K. Robinson, D.G. Mutch, C. Siegel, and Q. Zhu, "Evaluation of Ovarian Cancer: Initial Application of Coregistered Photoacoustic Tomography and US," Radiology **289**(3), 740–747 (2018).

[51] Y. Lin, P. Andreae, Z. Li, J. Cai, and H. Li, "Real-time co-registered photoacoustic and ultrasonic imaging for early endometrial cancer detection driven by cylindrical diffuser," J. Innov. Opt. Health Sci. **12**(02), 1950002 (2019).

[52] Y. Lin, R. Zheng, X. Zhang, Z. Li, and H. Li, "Image enhancement of photoacoustic imaging for early endometrial cancer detection by employing a filtered delay multiply and sum beamforming algorithm," AIP Advances **9**(12), 125303 (2019).

[53] C. Lu, K. Xiong, Y. Ma, W. Zhang, Z. Cheng, and S. Yang, "Electrothermal-MEMS-induced nonlinear distortion correction in photoacoustic laparoscopy," Opt. Express, OE **28**(10), 15300–15313 (2020).

[54] L. Xi, S.R. Grobmyer, L. Wu, R. Chen, G. Zhou, L.G. Gutwein, J. Sun, W. Liao, Q. Zhou, H. Xie, and H. Jiang, "Evaluation of breast tumor margins in vivo with intraoperative photoacoustic imaging," Opt. Express, OE **20**(8), 8726–8731 (2012).

[55] L.V. Wang, and S. Hu, "Photoacoustic Tomography: In Vivo Imaging from Organelles to Organs," Science **335**(6075), 1458–1462 (2012).

[56] K. Xiong, W. Wang, T. Guo, Z. Yuan, and S. Yang, "Shape-adapting panoramic photoacoustic endomicroscopy," Opt. Lett., OL **44**(11), 2681–2684 (2019).

[57] K. Xiong, S. Yang, X. Li, and D. Xing, "Autofocusing optical-resolution photoacoustic endoscopy," Opt. Lett., OL **43**(8), 1846–1849 (2018).

[58] G. Li, Z. Guo, and S.-L. Chen, "Miniature Probe for Forward-View Wide-Field Optical-Resolution Photoacoustic Endoscopy," IEEE Sensors Journal **19**(3), 909–916 (2019).

[59] L. Xi, J. Sun, Y. Zhu, L. Wu, H. Xie, and H. Jiang, "Photoacoustic imaging based on MEMS mirror scanning," Biomed. Opt. Express, BOE **1**(5), 1278–1283 (2010).

[60] Y. Li, X. Gong, C. Liu, R. Lin, W. Hau, X. Bai, and L. Song, "High-speed intravascular spectroscopic photoacoustic imaging at 1000 A-lines per second with a 0.9-mm diameter catheter," JBO **20**(6), 065006 (2015).

[61] B. Wang, A. Karpiouk, D. Yeager, J. Amirian, S. Litovsky, R. Smalling, and S. Emelianov, "*In vivo* Intravascular Ultrasound-guided Photoacoustic Imaging of Lipid in Plaques Using an Animal Model of Atherosclerosis," Ultrasound in Medicine & Biology **38**(12), 2098–2103 (2012).

[62] R. Virmani, A.P. Burke, F.D. Kolodgie, and A. Farb, "Pathology of the thin-cap fibroatheroma: a type of vulnerable plaque," J Interv Cardiol **16**(3), 267–272 (2003).

[63] M.T. Myaing, D.J. MacDonald, and X. Li, "Fiber-optic scanning two-photon fluorescence endoscope," Opt. Lett., OL **31**(8), 1076–1078 (2006).

[64] D. Ke, L. Wang, E. Wang, H. Xin, S. Yang, and K. Xiong, "Miniature fiber scanning probe for flexible forward-view photoacoustic endoscopy," Applied Physics Letters **122**(12), (2023).

[65] A. Seki, K. Iwai, T. Katagiri, and Y. Matsuura, "Forward-viewing photoacoustic imaging probe with bundled ultra-thin hollow optical fibers," J. Opt. **18**(7), 074015 (2016).

[66] A. Seki, K. Iwai, T. Katagiri, and Y. Matsuura, "Sensitivity improvement of optical fiber acoustic probe for all-optical photoacoustic imaging system," Appl. Phys. Express **10**(7), 072503 (2017).

[67] Y. Miida, and Y. Matsuura, "All-optical photoacoustic imaging system using fiber ultrasound probe and hollow optical fiber bundle," Opt. Express, OE **21**(19), 22023–22033 (2013).

[68] F. Zhong, and S. Hu, "Thin-film optical-acoustic combiner enables high-speed wide-field multi-parametric photoacoustic microscopy in reflection mode," Opt. Lett., OL **48**(2), 195–198 (2023).

[69] G. Oh, E. Chung, and S.H. Yun, "Optical fibers for high-resolution in vivo microendoscopic fluorescence imaging," Optical Fiber Technology **19**(6, Part B), 760–771 (2013).

[70] H. Cao, T. Čižmár, S. Turtaev, T. Tyc, and S. Rotter, "Controlling light propagation in multimode fibers for imaging, spectroscopy, and beyond," Adv. Opt. Photon., AOP **15**(2), 524–612 (2023).

[71] Antonio M. Caravaca-Aguirre, Sakshi Singh, Simon Labouesse, Michael V. Baratta, Rafael Piestun, and Emmanuel Bossy, "Hybrid photoacoustic-fluorescence microendoscopy through a multimode fiber using speckle illumination," APL Photonics **4**(9), 096103 (2019).

[72] T. Zhao, M.T. Ma, S. Ourselin, T. Vercauteren, and W. Xia, "Video-rate dual-modal photoacoustic and fluorescence imaging through a multimode fibre towards forward-viewing endomicroscopy," Photoacoustics **25**, 100323 (2022).

[73] T. Zhao, M. Zhang, S. Ourselin, and W. Xia, "Wavefront Shaping-Assisted Forward-Viewing Photoacoustic Endomicroscopy Based on a Transparent Ultrasound Sensor," Applied Sciences **12**(24), 12619 (2022).

[74] T. Zhao, T.T. Pham, C. Baker, M.T. Ma, S. Ourselin, T. Vercauteren, E. Zhang, P.C. Beard, and W. Xia, "Ultrathin, high-speed, all-optical photoacoustic endomicroscopy probe for guiding minimally invasive surgery," Biomed. Opt. Express **13**(8), 4414–4428 (2022).

[75] Ioannis N. Papadopoulos, Olivier Simandoux, Salma Farahi, Jean Pierre Huignard, Emmanuel Bossy, Demetri Psaltis, and Christophe Moser, "Optical-resolution photoacoustic microscopy by use of a multimode fiber," Appl. Phys. Lett. **102**(21), 211106 (2013).

[76] S. Mezil, A.M. Caravaca-Aguirre, E.Z. Zhang, P. Moreau, I. Wang, P.C. Beard, and E. Bossy, "Single-shot hybrid photoacoustic-fluorescent microendoscopy through a multimode fiber with wavefront shaping," Biomed. Opt. Express **11**(10), 5717–5727 (2020).

[77] A.M. Caravaca-Aguirre, F. Poisson, D. Bouchet, N. Stasio, P. Moreau, I. Wang, E. Zhang, P. Beard, C. Prada, C. Moser, D. Psaltis, O. Katz, and E. Bossy, "Single-Pixel Photoacoustic Microscopy with Speckle Illumination," Intelligent Computing **2**, 0011 (2023).

[78] A. Meiri, E.M. Strohm, M.C. Kolios, and Z. Zalevsky, "Spatial interference encoding patterns based photoacoustic microscopy," Optics Communications **401**, 23–28 (2017).

[79] R. Ansari, E.Z. Zhang, A.E. Desjardins, and P.C. Beard, "Miniature all-optical flexible forward-viewing photoacoustic endoscopy probe for surgical guidance," Opt. Lett., OL **45**(22), 6238–6241 (2020).

[80] M. Basij, Y. Yan, S.S. Alshahrani, H. Helmi, T.K. Burton, J.W. Burmeister, M.M. Dominello, I.S. Winer, and M. Mehrmohammadi, "Miniaturized phased-array ultrasound and photoacoustic endoscopic imaging system," Photoacoustics **15**, 100139 (2019).

[81] R. Ansari, E.Z. Zhang, A.E. Desjardins, and P.C. Beard, "All-optical forward-viewing photoacoustic probe for high-resolution 3D endoscopy," Light Sci Appl **7**(1), 75 (2018).

[82] A. Dangi, S. Agrawal, S. Tiwari, S. Jadhav, C. Cheng, G.R. Datta, S. Trolier-McKinstry, R. Pratap, and S.-R. Kothapalli, "Ring PMUT array based miniaturized photoacoustic endoscopy device," in *Photons Plus Ultrasound: Imaging and Sensing 2019*, (SPIE, 2019), pp. 46–53.

[83] D. Ren, C. Li, J. Shi, and R. Chen, "A Review of High-Frequency Ultrasonic Transducers for Photoacoustic Imaging Applications," IEEE Transactions on Ultrasonics, Ferroelectrics, and Frequency Control **69**(6), 1848–1858 (2022).

[84] Q. Zhou, X. Xu, E.J. Gottlieb, L. Sun, J.M. Cannata, H. Ameri, M.S. Humayun, P. Han, and K.K. Shung, "PMN-PT single crystal, high-frequency ultrasonic needle transducers for pulsed-wave Doppler application," IEEE Transactions on Ultrasonics, Ferroelectrics, and Frequency Control **54**(3), 668–675 (2007).

[85] W. Qi, R. Li, T. Ma, K. Kirk Shung, Q. Zhou, and Z. Chen, "Confocal acoustic radiation force optical coherence elastography using a ring ultrasonic transducer," Applied Physics Letters **104**(12), 123702 (2014).

[86] D. Ren, Y. Sun, J. Shi, and R. Chen, "A Review of Transparent Sensors for Photoacoustic Imaging Applications," Photonics **8**(8), 324 (2021).

[87] D.C. Garrett, and L.V. Wang, "Acoustic sensing with light," Nature Photonics, (2021).

[88] R. Shnaiderman, G. Wissmeyer, O. Ülgen, Q. Mustafa, A. Chmyrov, and V. Ntziachristos, "A submicrometre silicon-on-insulator resonator for ultrasound detection," Nature **585**(7825), 372–378 (2020).

[89] B. Dong, S. Chen, Z. Zhang, C. Sun, and H.F. Zhang, "Photoacoustic probe using a microring resonator ultrasonic sensor for endoscopic applications," Opt. Lett., OL **39**(15), 4372–4375 (2014).

[90] J. Pan, Q. Li, Y. Feng, R. Zhong, Z. Fu, S. Yang, W. Sun, B. Zhang, Q. Sui, J. Chen, Y. Shen, and Z. Li, "Parallel interrogation of the chalcogenide-based micro-ring sensor array for photoacoustic tomography," Nat Commun **14**(1), 3250 (2023).

[91] B. Dong, C. Sun, and H. F. Zhang, "Optical Detection of Ultrasound in Photoacoustic Imaging," IEEE Transactions on Biomedical Engineering **64**(1), 4–15 (2017).

[92] G. Wissmeyer, M.A. Pleitez, A. Rosenthal, and V. Ntziachristos, "Looking at sound: optoacoustics with all-optical ultrasound detection," Light: Science & Applications **7**(1), 53 (2018).

[93] J. Jung, W. Lee, W. Kang, E. Shin, J. Ryu, and H. Choi, "Review of piezoelectric micromachined ultrasonic transducers and their applications," J. Micromech. Microeng. **27**(11), 113001 (2017).

[94] K. Brenner, A.S. Ergun, K. Firouzi, M.F. Rasmussen, Q. Stedman, and B. (Pierre) Khuri–Yakub, "Advances in Capacitive Micromachined Ultrasonic Transducers," Micromachines **10**(2), 152 (2019).

[95] A.K. Ilkhechi, C. Ceroici, Z. Li, and R. Zemp, "Transparent capacitive micromachined ultrasonic transducer (CMUT) arrays for real-time photoacoustic applications," Opt. Express, OE **28**(9), 13750–13760 (2020).

[96] S. Vaithilingam, T.-J. Ma, Y. Furukawa, I.O. Wygant, X. Zhuang, A. De La Zerda, O. Oralkan, A. Kamaya, S. s. Gambhir, R.B. Jeffrey, and B.T. Khuri-yakub, "Three-dimensional photoacoustic imaging using a two-dimensional CMUT array," IEEE Transactions on Ultrasonics, Ferroelectrics, and Frequency Control **56**(11), 2411–2419 (2009).

[97] A. Dangi, C.Y. Cheng, S. Agrawal, S. Tiwari, G.R. Datta, R.R. Benoit, R. Pratap, S. Trolier-Mckinstry, and S.-R. Kothapalli, "A Photoacoustic Imaging Device Using Piezoelectric Micromachined Ultrasound Transducers (PMUTs)," IEEE Transactions on Ultrasonics, Ferroelectrics, and Frequency Control **67**(4), 801–809 (2020).

[98] Q. Zheng, H. Wang, H. Yang, H. Jiang, Z. Chen, Y. Lu, P.X.-L. Feng, and H. Xie, "Thin ceramic PZT dual- and multi-frequency pMUT arrays for photoacoustic imaging," Microsyst Nanoeng **8**(1), 1–12 (2022).

[99] J. Cai, Y. Wang, D. Jiang, S. Zhang, Y.A. Gu, L. Lou, F. Gao, and T. Wu, "Beyond fundamental resonance mode: high-order multi-band ALN PMUT for in vivo photoacoustic imaging," Microsyst Nanoeng **8**(1), 1–12 (2022).

[100] M.S. Salim, M.F. Abd Malek, R.B.W. Heng, K.M. Juni, and N. Sabri, "Capacitive Micromachined Ultrasonic Transducers: Technology and Application," Journal of Medical Ultrasound **20**(1), 8–31 (2012).

[101] J.-M. Yang, R. Chen, C. Favazza, J. Yao, C. Li, Z. Hu, Q. Zhou, K.K. Shung, and L.V. Wang, "A 2.5-mm diameter probe for photoacoustic and ultrasonic endoscopy," Opt. Express, OE **20**(21), 23944–23953 (2012).

[102] J.-M. Yang, C. Li, R. Chen, Q. Zhou, K.K. Shung, and L.V. Wang, "Catheter-based photoacoustic endoscope," JBO **19**(6), 066001 (2014).

[103] J.A. Guggenheim, J. Li, T.J. Allen, R.J. Colchester, S. Noimark, O. Ogunlade, I.P. Parkin, I. Papakonstantinou, A.E. Desjardins, E.Z. Zhang, and P.C. Beard, "Ultrasensitive plano-concave optical microresonators for ultrasound sensing," Nature Photonics **11**(11), 714–719 (2017).

[104] H. Li, B. Dong, X. Zhang, X. Shu, X. Chen, R. Hai, D.A. Czaplewski, H.F. Zhang, and C. Sun, "Disposable ultrasound-sensing chronic cranial window by soft nanoimprinting lithography," Nature Communications **10**(1), 4277 (2019).

[105] Y. Liang, L. Jin, L. Wang, X. Bai, L. Cheng, and B.-O. Guan, "Fiber-Laser-Based Ultrasound Sensor for Photoacoustic Imaging," Scientific Reports **7**(1), 40849 (2017).

[106] C. Liu, and L. Wang, "Functional photoacoustic microscopy of hemodynamics: a review," Biomed. Eng. Lett. **12**(2), 97–124 (2022).

[107] H.F. Zhang, K. Maslov, M. Sivaramakrishnan, G. Stoica, and L.V. Wang, "Imaging of hemoglobin oxygen saturation variations in single vessels in vivo using photoacoustic microscopy," Applied Physics Letters **90**(5), 053901 (2007).

[108] Z. Xu, N. Sun, R. Cao, Z. Li, Q. Liu, and S. Hu, "Cortex-wide multiparametric photoacoustic microscopy based on real-time contour scanning," NPh **6**(3), 035012 (2019).

[109] K. Jansen, A.F.W. van der Steen, M. Wu, H.M.M. van Beusekom, G. Springeling, X. Li, Q. Zhou, K.K. Shung, D.P. de Kleijn, and G. van Soest, "Spectroscopic intravascular photoacoustic imaging of lipids in atherosclerosis," JBO **19**(2), 026006 (2014).

[110] J. Zhang, S. Yang, X. Ji, Q. Zhou, and D. Xing, "Characterization of Lipid-Rich Aortic Plaques by Intravascular Photoacoustic Tomography: Ex Vivo and In Vivo Validation in a Rabbit Atherosclerosis Model With Histologic Correlation," Journal of the American College of Cardiology **64**(4), 385–390 (2014).

[111] Z. Wang, Y. Zhou, and S. Hu, "Sparse Coding-Enabled Low-Fluence Multi-Parametric Photoacoustic Microscopy," IEEE Transactions on Medical Imaging **41**(4), 805–814 (2022).

[112] A. Danielli, C.P. Favazza, K. Maslov, and L.V. Wang, "Picosecond absorption relaxation measured with nanosecond laser photoacoustics," Applied Physics Letters **97**(16), 163701 (2010).

[113] A. Danielli, C.P. Favazza, K. Maslov, and L.V. Wang, "Single-wavelength functional photoacoustic microscopy in biological tissue," Opt. Lett., OL **36**(5), 769–771 (2011).

[114] J. Yao, L. Wang, J.-M. Yang, K.I. Maslov, T.T.W. Wong, L. Li, C.-H. Huang, J. Zou, and L.V. Wang, "High-speed label-free functional photoacoustic microscopy of mouse brain in action," Nat Methods **12**(5), 407–410 (2015).

[115] G.P. Agrawal, "Nonlinear Fiber Optics," in *Nonlinear Science at the Dawn of the 21st Century*, edited by P.L. Christiansen, M.P. Sørensen, and A.C. Scott, (Springer, Berlin, Heidelberg, 2000), pp. 195–211.

[116] C. Liu, J. Chen, Y. Zhang, J. Zhu, and L. Wang, "Five-wavelength optical-resolution photoacoustic microscopy of blood and lymphatic vessels," AP **3**(1), 016002 (2021).

[117] S. Mirg, K.L. Turner, H. Chen, P.J. Drew, and S.-R. Kothapalli, "Photoacoustic imaging for microcirculation," Microcirculation **29**(6–7), e12776 (2022).

[118] S. Kou, X. Leng, H. Luo, H. Nie, and Q. Zhu, "Acoustic resolution photoacoustic Doppler flowmetry for assessment of patient rectal cancer blood perfusion," JBO **29**(S1), S11517 (2024).

[119] J. Yao, and L.V. Wang, "Transverse flow imaging based on photoacoustic Doppler bandwidth broadening," JBO **15**(2), 021304 (2010).

[120] S.-L. Chen, T. Ling, S.-W. Huang, H.W. Baac, and L.J. Guo, "Photoacoustic correlation spectroscopy and its application to low-speed flow measurement," Opt. Lett., OL **35**(8), 1200–1202 (2010).

[121] J. Brunker, and P. Beard, "Pulsed photoacoustic Doppler flowmetry using time-domain cross-correlation: Accuracy, resolution and scalability," The Journal of the Acoustical Society of America **132**(3), 1780–1791 (2012).

[122] C. Liu, Y. Liang, and L. Wang, "Single-shot photoacoustic microscopy of hemoglobin concentration, oxygen saturation, and blood flow in sub-microseconds," Photoacoustics **17**, 100156 (2020).

[123] W. Liu, B. Lan, L. Hu, R. Chen, Q. Zhou, and J. Yao, "Photoacoustic thermal flowmetry with a single light source," JBO **22**(9), 096001 (2017).

[124] D. Zhang, L. Men, and Q. Chen, "Femtosecond laser fabricated polymer microring resonator for sensing applications," Electronics Letters **54**(14), 888–890 (2018).

[125] E.A. Kiyatkin, "Brain temperature and its role in physiology and pathophysiology: Lessons from 20 years of thermorecording," Temperature **6**(4), 271–333 (2019).

[126] Y. Zhou, M. Li, W. Liu, G. Sankin, J. Luo, P. Zhong, and J. Yao, "Thermal memory based photoacoustic imaging of temperature," Optica, OPTICA **6**(2), 198–205 (2019).

[127] S. Xie, "Chapter Twenty-One - MR OEF Imaging in MELAS," in *Methods in Enzymology*, edited by A.N. Murphy and D.C. Chan, (Academic Press, 2014), pp. 433–444.

[128] J. Chen, Y. Zhang, X. Li, J. Zhu, D. Li, S. Li, C.-S. Lee, and L. Wang, "Confocal visible/NIR photoacoustic microscopy of tumors with structural, functional, and nanoprobe contrasts," Photon. Res., PRJ **8**(12), 1875–1880 (2020).

[129] S. Hu, E. Gonzales, B. Soetikno, E. Gong, P. Yan, K. Maslov, J.-M. Lee, and L.V. Wang, "Optical-resolution photoacoustic microscopy of ischemic stroke," in *Photons Plus Ultrasound: Imaging and Sensing 2011*, (SPIE, 2011), pp. 41–45.

[130] A. Farooq, S. Sabah, S. Dhou, N. Alsawaftah, and G. Husseini, "Exogenous Contrast Agents in Photoacoustic Imaging: An In Vivo Review for Tumor Imaging," Nanomaterials **12**(3), 393 (2022).

[131] G.P. Luke, D. Yeager, and S.Y. Emelianov, "Biomedical Applications of Photoacoustic Imaging with Exogenous Contrast Agents," Ann Biomed Eng **40**(2), 422–437 (2012).

[132] Z. Chen, I. Gezginer, Q. Zhou, L. Tang, X.L. Deán-Ben, and D. Razansky, "Multimodal optoacoustic imaging: methods and contrast materials," Chem. Soc. Rev., (2024).

[133] G. Keiser, *Optical Fiber Communications* (McGraw-Hill, 2000).

[134] R. Kingslake, *Lens Design Fundamentals* (Elsevier, 2012).

[135] D.C. Leiner, and R. Prescott, "Correction of chromatic aberrations in GRIN endoscopes," Appl. Opt., AO **22**(3), 383–386 (1983).

[136] C. Markos, J.C. Travers, A. Abdolvand, B.J. Eggleton, and O. Bang, "Hybrid photonic-crystal fiber," Rev. Mod. Phys. **89**(4), 045003 (2017).

[137] L. Fu, A. Jain, H. Xie, C. Cranfield, and M. Gu, "Nonlinear optical endoscopy based on a double-clad photonic crystal fiber and a MEMS mirror," Opt. Express, OE **14**(3), 1027–1032 (2006).

[138] D. Septier, V. Mytskaniuk, R. Habert, D. Labat, K. Baudelle, A. Cassez, G. Brévalle-Wasilewski, M. Conforti, G. Bouwmans, H. Rigneault, and A. Kudlinski, "Label-free highly multimodal nonlinear endoscope," Opt. Express, OE **30**(14), 25020–25033 (2022).

[139] V. Kučikas, M.P. Werner, T. Schmitz-Rode, F. Louradour, and M.A.M.J. van Zandvoort, "Two-Photon Endoscopy: State of the Art and Perspectives," Mol Imaging Biol **25**(1), 3–17 (2023).

[140] T.A. Birks, J.C. Knight, and P.S.J. Russell, "Endlessly single-mode photonic crystal fiber," Opt. Lett., OL **22**(13), 961–963 (1997).

[141] J.C. Knight, T.A. Birks, R.F. Cregan, P.S.J. Russell, and J.P. de Sandro, "Large mode area photonic crystal fibre," Electronics Letters **34**(13), 1347–1348 (1998).

[142] C. Wei, R.J. Weiblen, C.R. Menyuk, and J. Hu, "Negative curvature fibers," Adv. Opt. Photon., AOP **9**(3), 504–561 (2017).

[143] F. Benabid, and P.J. Roberts, "Linear and nonlinear optical properties of hollow core photonic crystal fiber," Journal of Modern Optics **58**(2), 87–124 (2011).

[144] G. Humbert, J.C. Knight, G. Bouwmans, P.S.J. Russell, D.P. Williams, P.J. Roberts, and B.J. Mangan, "Hollow core photonic crystal fibers for beam delivery," Opt. Express, OE **12**(8), 1477–1484 (2004).

[145] K.-S. Lee, R.H. Kim, D.-Y. Yang, and S.H. Park, "Advances in 3D nano/microfabrication using two-photon initiated polymerization," Progress in Polymer Science **33**(6), 631–681 (2008).

[146] D. Gonzalez-Hernandez, S. Varapnickas, A. Bertoncini, C. Liberale, and M. Malinauskas, "Micro-Optics 3D Printed via Multi-Photon Laser Lithography," Advanced Optical Materials **11**(1), 2201701 (2023).

[147] H. Wang, W. Zhang, D. Ladika, H. Yu, D. Gailevičius, H. Wang, C.-F. Pan, P.N.S. Nair, Y. Ke, T. Mori, J.Y.E. Chan, Q. Ruan, M. Farsari, M. Malinauskas, S. Juodkazis, M. Gu, and J.K.W. Yang, "Two-Photon Polymerization Lithography for Optics and Photonics: Fundamentals, Materials, Technologies, and Applications," Advanced Functional Materials **33**(39), 2214211 (2023).

[148] P. Somers, A. Münchinger, S. Maruo, C. Moser, X. Xu, and M. Wegener, "The physics of 3D printing with light," Nat Rev Phys, 1–15 (2023).

[149] K. Obata, J. Koch, U. Hinze, and B.N. Chichkov, "Multi-focus two-photon polymerization technique based on individually controlled phase modulation," Opt. Express, OE **18**(16), 17193–17200 (2010).

[150] P. Somers, Z. Liang, J.E. Johnson, B.W. Boudouris, L. Pan, and X. Xu, "Rapid, continuous projection multi-photon 3D printing enabled by spatiotemporal focusing of femtosecond pulses," Light Sci Appl **10**(1), 199 (2021).

[151] C. Liberale, G. Cojoc, P. Candeloro, G. Das, F. Gentile, F. De Angelis, and E. Di Fabrizio, "Micro-Optics Fabrication on Top of Optical Fibers Using Two-Photon Lithography," IEEE Photonics Technology Letters **22**(7), 474–476 (2010).

[152] R. Guo, S. Xiao, X. Zhai, J. Li, A. Xia, and W. Huang, "Micro lens fabrication by means of femtosecond two photon photopolymerization," Opt. Express, OE **14**(2), 810–816 (2006).

[153] M. Malinauskas, A. Žukauskas, V. Purlys, K. Belazaras, A. Momot, D. Paipulas, R. Gadonas, A. Piskarskas, H. Gilbergs, A. Gaidukevičiūtė, I. Sakellari, M. Farsari, and S. Juodkazis, "Femtosecond laser polymerization of hybrid/integrated micro-optical elements and their characterization," J. Opt. **12**(12), 124010 (2010).

[154] T. Gissibl, S. Thiele, A. Herkommer, and H. Giessen, "Two-photon direct laser writing of ultracompact multi-lens objectives," Nature Photon **10**(8), 554–560 (2016).

[155] U.T. Sanli, H. Ceylan, I. Bykova, M. Weigand, M. Sitti, G. Schütz, and K. Keskinbora, "3D Nanoprinted Plastic Kinoform X-Ray Optics," Advanced Materials **30**(36), 1802503 (2018).

[156] S. Thiele, C. Pruss, A.M. Herkommer, and H. Giessen, "3D printed stacked diffractive microlenses," Opt. Express, OE **27**(24), 35621–35630 (2019).

[157] H. Wang, H. Wang, W. Zhang, and J.K.W. Yang, "Toward Near-Perfect Diffractive Optical Elements via Nanoscale 3D Printing," ACS Nano **14**(8), 10452–10461 (2020).

[158] L. Yan, D. Yang, Q. Gong, and Y. Li, "Rapid Fabrication of Continuous Surface Fresnel Microlens Array by Femtosecond Laser Focal Field Engineering," Micromachines **11**(2), 112 (2020).

[159] W. Hadibrata, H. Wei, S. Krishnaswamy, and K. Aydin, "Inverse Design and 3D Printing of a Metalens on an Optical Fiber Tip for Direct Laser Lithography," Nano Lett. **21**(6), 2422–2428 (2021).

[160] F. Balli, M.A. Sultan, A. Ozdemir, and J.T. Hastings, "An ultrabroadband 3D achromatic metalens," Nanophotonics **10**(4), 1259–1264 (2021).

[161] C.-F. Pan, H. Wang, H. Wang, P.N. S, Q. Ruan, S. Wredh, Y. Ke, J.Y.E. Chan, W. Zhang, C.-W. Qiu, and J.K.W. Yang, "3D-printed multilayer structures for high–numerical aperture achromatic metalenses," Science Advances **9**(51), eadj9262 (2023).

[162] M. Schmid, F. Sterl, S. Thiele, A. Herkommer, and H. Giessen, "3D printed hybrid refractive/diffractive achromat and apochromat for the visible wavelength range," Opt. Lett., OL **46**(10), 2485–2488 (2021).

[163] J. Li, P. Fejes, D. Lorenser, B.C. Quirk, P.B. Noble, R.W. Kirk, A. Orth, F.M. Wood, B.C. Gibson, D.D. Sampson, and R.A. McLaughlin, "Two-photon polymerisation 3D printed freeform micro-optics for optical coherence tomography fibre probes," Sci Rep **8**(1), 14789 (2018).

[164] J. Li, S. Thiele, B.C. Quirk, R.W. Kirk, J.W. Verjans, E. Akers, C.A. Bursill, S.J. Nicholls, A.M. Herkommer, H. Giessen, and R.A. McLaughlin, "Ultrathin monolithic 3D printed optical coherence tomography endoscopy for preclinical and clinical use," Light Sci Appl **9**(1), 124 (2020).

[165] J. Li, S. Thiele, R.W. Kirk, B.C. Quirk, A. Hoogendoorn, Y.C. Chen, K. Peter, S.J. Nicholls, J.W. Verjans, P.J. Psaltis, C. Bursill, A.M. Herkommer, H. Giessen, and R.A. McLaughlin, "3D-Printed Micro Lens-in-Lens for In Vivo Multimodal Microendoscopy," Small **18**(17), 2107032 (2022).

[166] S. Gigan, O. Katz, H.B. de Aguiar, E.R. Andresen, A. Aubry, J. Bertolotti, E. Bossy, D. Bouchet, J. Brake, S. Brasselet, Y. Bromberg, H. Cao, T. Chaigne, Z. Cheng, W. Choi, T. Čižmár, M. Cui, V.R. Curtis, H. Defienne, M. Hofer, R. Horisaki, R. Horstmeyer, N. Ji, A.K. LaViolette, J. Mertz, C. Moser, A.P. Mosk, N.C. Pégard, R. Piestun, S. Popoff, D.B. Phillips, D. Psaltis, B. Rahmani, H. Rigneault, S. Rotter, L. Tian, I.M. Vellekoop, L. Waller, L. Wang, T. Weber, S. Xiao, C. Xu, A. Yamilov, C. Yang, and H. Yılmaz, "Roadmap on wavefront shaping and deep imaging in complex media," J. Phys. Photonics **4**(4), 042501 (2022).

[167] S.-Y. Lee, V.J. Parot, B.E. Bouma, and M. Villiger, "Confocal 3D reflectance imaging through multimode fiber without wavefront shaping," Optica, OPTICA **9**(1), 112–120 (2022).

[168] S. Turtaev, I.T. Leite, K.J. Mitchell, M.J. Padgett, D.B. Phillips, and T. Čižmár, "Comparison of nematic liquid-crystal and DMD based spatial light modulation in complex photonics," Opt. Express, OE **25**(24), 29874–29884 (2017).

[169] B. Ning, M.J. Kennedy, A.J. Dixon, N. Sun, R. Cao, B.T. Soetikno, R. Chen, Q. Zhou, K.K. Shung, J.A. Hossack, and S. Hu, "Simultaneous photoacoustic microscopy of microvascular anatomy, oxygen saturation, and blood flow," Opt. Lett., OL **40**(6), 910–913 (2015).

[170] R. Cao, J. Li, B. Ning, N. Sun, T. Wang, Z. Zuo, and S. Hu, "Functional and oxygen-metabolic photoacoustic microscopy of the awake mouse brain," NeuroImage **150**, 77–87 (2017).

[171] S. Turtaev, I.T. Leite, T. Altwegg-Boussac, J.M.P. Pakan, N.L. Rochefort, and T. Čižmár, "High-fidelity multimode fibre-based endoscopy for deep brain in vivo imaging," Light: Science & Applications **7**(1), 92 (2018).

[172] T. Zhao, S. Ourselin, T. Vercauteren, and W. Xia, "Seeing through multimode fibers with real-valued intensity transmission matrices," Opt. Express **28**(14), 20978–20991 (2020).
[173] O. Tzang, E. Niv, S. Singh, S. Labouesse, G. Myatt, and R. Piestun, "Wavefront shaping in complex media with a 350 kHz modulator via a 1D-to-2D transform," Nature Photonics **13**(11), 788–793 (2019).
[174] S. Farahi, D. Ziegler, I.N. Papadopoulos, D. Psaltis, and C. Moser, "Dynamic bending compensation while focusing through a multimode fiber," Opt. Express, OE **21**(19), 22504–22514 (2013).
[175] G.S.D. Gordon, M. Gataric, A.G.C.P. Ramos, R. Mouthaan, C. Williams, J. Yoon, T.D. Wilkinson, and S.E. Bohndiek, "Characterizing Optical Fiber Transmission Matrices Using Metasurface Reflector Stacks for Lensless Imaging without Distal Access," Phys. Rev. X **9**(4), 041050 (2019).
[176] H. Chen, N.K. Fontaine, R. Ryf, D.T. Neilson, and P. Winzer, "Remote Spatio-Temporal Focusing Over Multimode Fiber Enabled by Single-Ended Channel Estimation," IEEE Journal of Selected Topics in Quantum Electronics **26**(4), 1–9 (2020).
[177] S. Li, S.A.R. Horsley, T. Tyc, T. Čižmár, and D.B. Phillips, "Memory effect assisted imaging through multimode optical fibres," Nat Commun **12**(1), 3751 (2021).
[178] Z. Wen, Z. Dong, Q. Deng, C. Pang, C.F. Kaminski, X. Xu, H. Yan, L. Wang, S. Liu, J. Tang, W. Chen, X. Liu, and Q. Yang, "Single multimode fibre for in vivo light-field-encoded endoscopic imaging," Nat. Photon. **17**(8), 679–687 (2023).
[179] Y. Zheng, T. Wright, Z. Wen, Q. Yang, and G.S.D. Gordon, "Single-ended recovery of optical fiber transmission matrices using neural networks," Commun Phys **6**(1), 1–12 (2023).
[180] A. Mafi, J. Ballato, K.W. Koch, and A. Schülzgen, "Disordered Anderson Localization Optical Fibers for Image Transport—A Review," Journal of Lightwave Technology **37**(22), 5652–5659 (2019).
[181] S. Karbasi, R.J. Frazier, K.W. Koch, T. Hawkins, J. Ballato, and A. Mafi, "Image transport through a disordered optical fibre mediated by transverse Anderson localization," Nat Commun **5**(1), 3362 (2014).
[182] B. Abaie, M. Peysokhan, J. Zhao, J.E. Antonio-Lopez, R. Amezcua-Correa, A. Schülzgen, and A. Mafi, "Disorder-induced high-quality wavefront in an Anderson localizing optical fiber," Optica, OPTICA **5**(8), 984–987 (2018).
[183] J. Zhao, J.E.A. Lopez, Z. Zhu, D. Zheng, S. Pang, R.A. Correa, and A. Schülzgen, "Image Transport Through Meter-Long Randomly Disordered Silica-Air Optical Fiber," Sci Rep **8**(1), 3065 (2018).
[184] X. Hu, J. Zhao, J.E. Antonio-Lopez, R.A. Correa, and A. Schülzgen, "Unsupervised full-color cellular image reconstruction through disordered optical fiber," Light Sci Appl **12**(1), 125 (2023).
[185] X. Zhan, Z. Wang, S. Kumar, C. Marques, X. Li, and R. Min, "The Application of Pound–Drever–Hall Technology in High-Resolution Sensing—A Review," IEEE Sensors Journal **23**(7), 6427–6438 (2023).
[186] A. Rosenthal, D. Razansky, and V. Ntziachristos, "Wideband optical sensing using pulse interferometry," Opt. Express, OE **20**(17), 19016–19029 (2012).
[187] A. Rosenthal, S. Kellnberger, D. Bozhko, A. Chekkoury, M. Omar, D. Razansky, and V. Ntziachristos, "Sensitive interferometric detection of ultrasound for minimally invasive clinical imaging applications," Laser & Photonics Reviews **8**(3), 450–457 (2014).
[188] G. Wissmeyer, D. Soliman, R. Shnaiderman, A. Rosenthal, and V. Ntziachristos, "All-optical optoacoustic microscope based on wideband pulse interferometry," Opt. Lett. **41**(9), 1953–1956 (2016).
[189] A.L. Gaeta, M. Lipson, and T.J. Kippenberg, "Photonic-chip-based frequency combs," Nature Photon **13**(3), 158–169 (2019).

[190] X. Bai, Y. Liang, H. Sun, L. Jin, J. Ma, B.-O. Guan, and L. Wang, "Sensitivity characteristics of broadband fiber-laser-based ultrasound sensors for photoacoustic microscopy," Opt. Express **25**(15), 17616–17626 (2017).

[191] Y. Wang, C. Li, and R.K. Wang, "Noncontact photoacoustic imaging achieved by using a low-coherence interferometer as the acoustic detector," Opt. Lett., OL **36**(20), 3975–3977 (2011).

[192] A. Hochreiner, J. Bauer-Marschallinger, P. Burgholzer, B. Jakoby, and T. Berer, "Non-contact photoacoustic imaging using a fiber based interferometer with optical amplification," Biomed. Opt. Express, BOE **4**(11), 2322–2331 (2013).

[193] P. Hajireza, W. Shi, K. Bell, R.J. Paproski, and R.J. Zemp, "Non-interferometric photoacoustic remote sensing microscopy," Light: Science & Applications **6**(6), e16278–e16278 (2017).

[194] P.H. Reza, K. Bell, W. Shi, J. Shapiro, and R.J. Zemp, "Deep non-contact photoacoustic initial pressure imaging," Optica **5**(7), 814–820 (2018).

[195] J. Zhou, J. Zhou, W. Wang, S. Liang, L. Jing, S.-H. Bo, and S.-L. Chen, "Miniature non-contact photoacoustic probe based on fiber-optic photoacoustic remote sensing microscopy," Opt. Lett., OL **46**(22), 5767–5770 (2021).

[196] H. Zhao, Z. Ke, F. Yang, K. Li, N. Chen, L. Song, C. Zheng, D. Liang, and C. Liu, "Deep Learning Enables Superior Photoacoustic Imaging at Ultralow Laser Dosages," Advanced Science **8**(3), 2003097 (2021).

[197] P. Farnia, E. Najafzadeh, A. Hariri, S.N. Lavasani, B. Makkiabadi, A. Ahmadian, and J.V. Jokerst, "Dictionary learning technique enhances signal in LED-based photoacoustic imaging," Biomed. Opt. Express **11**(5), 2533–2547 (2020).

[198] I. Ul Haq, R. Nagaoka, S. Siregar, and Y. Saijo, "Sparse-representation-based denoising of photoacoustic images," Biomedical Physics & Engineering Express **3**(4), 045014 (2017).

[199] A.F. Kosolapov, G.K. Alagashev, A.N. Kolyadin, A.D. Pryamikov, A.S. Biryukov, I.A. Bufetov, and E.M. Dianov, "Hollow-core revolver fibre with a double-capillary reflective cladding," Quantum Electron. **46**(3), 267 (2016).

[200] J. Yao, "When pressure meets light: detecting the photoacoustic effect at the origin," Light Sci Appl **6**(6), e17062–e17062 (2017).

[201] Chimowitz Marc I., Lynn Michael J., Derdeyn Colin P., Turan Tanya N., Fiorella David, Lane Bethany F., Janis L. Scott, Lutsep Helmi L., Barnwell Stanley L., Waters Michael F., Hoh Brian L., Hourihane J. Maurice, Levy Elad I., Alexandrov Andrei V., Harrigan Mark R., Chiu David, Klucznik Richard P., Clark Joni M., McDougall Cameron G., Johnson Mark D., Pride G. Lee, Torbey Michel T., Zaidat Osama O., Rumboldt Zoran, and Cloft Harry J., "Stenting versus Aggressive Medical Therapy for Intracranial Arterial Stenosis," New England Journal of Medicine **365**(11), 993–1003 (2011).

[202] W. Brinjikji, M.H. Murad, G. Lanzino, H.J. Cloft, and D.F. Kallmes, "Endovascular Treatment of Intracranial Aneurysms With Flow Diverters," Stroke **44**(2), 442–447 (2013).

[203] C.R. Pasarikovski, J.C. Ku, S.M. Priola, L. da Costa, and V.X.D. Yang, "Endovascular optical coherence tomography imaging in cerebrovascular disease," Journal of Clinical Neuroscience **80**, 30–37 (2020).

[204] V. Anagnostakou, G.J. Ughi, A.S. Puri, and M.J. Gounis, "Optical Coherence Tomography for Neurovascular Disorders," Neuroscience **474**, 134–144 (2021).

[205] V.M. Pereira, P. Lylyk, N. Cancelliere, P.N. Lylyk, I. Lylyk, V. Anagnostakou, C. Bleise, H. Nishi, M. Epshtein, R.M. King, M.S. Shazeeb, A.S. Puri, C.W. Liang, R.A. Hanel, J. Spears, T.R. Marotta, D.K. Lopes, M.J. Gounis, and G.J. Ughi, "Volumetric microscopy of cerebral arteries with a miniaturized optical coherence tomography imaging probe," Science Translational Medicine **16**(747), eadl4497 (2024).

[206] G.J. Ughi, M.G. Marosfoi, R.M. King, J. Caroff, L.M. Peterson, B.H. Duncan, E.T. Langan, A. Collins, A. Leporati, S. Rousselle, D.K. Lopes, M.J. Gounis, and A.S. Puri, "A neurovascular high-frequency optical coherence tomography system enables in situ cerebrovascular volumetric microscopy," Nat Commun **11**(1), 3851 (2020).

[207] C.S. Ahuja, J.R. Wilson, S. Nori, M.R.N. Kotter, C. Druschel, A. Curt, and M.G. Fehlings, "Traumatic spinal cord injury," Nat Rev Dis Primers **3**(1), 1–21 (2017).

[208] V. Hubertus, L. Meyer, L. Roolfs, L. Waldmann, M. Nieminen-Kelhä, M.G. Fehlings, and P. Vajkoczy, "*In vivo* imaging in experimental spinal cord injury – Techniques and trends," Brain and Spine **2**, 100859 (2022).

[209] P.W. Stroman, C. Wheeler-Kingshott, M. Bacon, J.M. Schwab, R. Bosma, J. Brooks, D. Cadotte, T. Carlstedt, O. Ciccarelli, J. Cohen-Adad, A. Curt, N. Evangelou, M.G. Fehlings, M. Filippi, B.J. Kelley, S. Kollias, A. Mackay, C.A. Porro, S. Smith, S.M. Strittmatter, P. Summers, and I. Tracey, "The current state-of-the-art of spinal cord imaging: Methods," NeuroImage **84**, 1070–1081 (2014).

[210] D.W. Cadotte, A. Mariampillai, A. Cadotte, K.K.C. Lee, T.-R. Kiehl, B.C. Wilson, M.G. Fehlings, and V.X.D. Yang, "Speckle variance optical coherence tomography of the rodent spinal cord: in vivo feasibility," Biomed. Opt. Express, BOE **3**(5), 911–919 (2012).

[211] S.A. Figley, Y. Chen, A. Maeda, L. Conroy, J.D. McMullen, J.I. Silver, S. Stapleton, A. Vitkin, P. Lindsay, K. Burrell, G. Zadeh, M.G. Fehlings, and R.S. DaCosta, "A Spinal Cord Window Chamber Model for In Vivo Longitudinal Multimodal Optical and Acoustic Imaging in a Murine Model," PLOS ONE **8**(3), e58081 (2013).

[212] T.Y.E. Ahmadieh, E.M. Wu, B. Kafka, J.P. Caruso, O.J. Neeley, A. Plitt, S.G. Aoun, D.M. Olson, R.A. Ruchinskas, C.M. Cullum, S. Barnett, B.G. Welch, H.H. Batjer, and J.A. White, "Lumbar drain trial outcomes of normal pressure hydrocephalus: a single-center experience of 254 patients," Journal of Neurosurgery **132**(1), 306–312 (2019).

[213] C.R. Pasarikovski, J.C. Ku, J. Ramjist, Y. Dobashi, S.M. Priola, L. da Costa, A. Kumar, and V.X.D. Yang, "Minimally invasive intrathecal spinal cord imaging with optical coherence tomography," JBO **26**(5), 056002 (2021).

[214] J. Raskin, J. Cummings, J. Hardy, K. Schuh, and R.A. Dean, "Neurobiology of Alzheimer's Disease: Integrated Molecular, Physiological, Anatomical, Biomarker, and Cognitive Dimensions," Curr Alzheimer Res **12**(8), 712–722 (2015).

[215] F. Han, "Cerebral microvascular dysfunction and neurodegeneration in dementia," Stroke Vasc Neurol **4**(2), (2019).

[216] R. Cao, J. Li, C. Zhang, Z. Zuo, and S. Hu, "Photoacoustic microscopy of obesity-induced cerebrovascular alterations," NeuroImage **188**, 369–379 (2019).

[217] A.P. Slovinski, L.A. Hajjar, and C. Ince, "Microcirculation in Cardiovascular Diseases," J Cardiothorac Vasc Anesth **33**(12), 3458–3468 (2019).

[218] L. Lin, X. Tong, S. Cavallero, Y. Zhang, S. Na, R. Cao, T.K. Hsiai, and L.V. Wang, "Non-invasive photoacoustic computed tomography of rat heart anatomy and function," Light Sci Appl **12**(1), 12 (2023).

[219] J. Chen, Y. Zhang, J. Zhu, X. Tang, and L. Wang, "Freehand scanning photoacoustic microscopy with simultaneous localization and mapping," Photoacoustics **28**, 100411 (2022).

[220] K. Jung, P. Kim, F. Leuschner, R. Gorbatov, J.K. Kim, T. Ueno, M. Nahrendorf, and S.H. Yun, "Endoscopic time-lapse imaging of immune cells in infarcted mouse hearts," Circ Res **112**(6), 891–899 (2013).

[221] S. Lee, C. Vinegoni, P.F. Feruglio, L. Fexon, R. Gorbatov, M. Pivoravov, A. Sbarbati, M. Nahrendorf, and R. Weissleder, "Real-time in vivo imaging of the beating mouse heart at microscopic resolution," Nat Commun **3**(1), 1054 (2012).